MOLECULAR AND CELLULAR BIOLOGY, June 2009, p. 3186–3203 Vol. 29, No. 11
0270-7306/09/$08.00+0 doi:10.1128/MCB.01970-08

The Pluripotency-Associated Gene *Dppa4* Is Dispensable for Embryonic Stem Cell Identity and Germ Cell Development but Essential for Embryogenesis▽†

Babita Madan,[1] Vikas Madan,[1] Odile Weber,[1] Philippe Tropel,[2,3] Carmen Blum,[1] Emmanuelle Kieffer,[2] Stéphane Viville,[2] and Hans Jörg Fehling[1]*

Institute of Immunology, University Clinics Ulm, Albert Einstein Allee 11, D-89081 Ulm, Germany,[1] and Institut de Génétique et de Biologie Moléculaire et Cellulaire, B.P. 10142, F-67404 Strasbourg-Illkirch,[2] and I-STEM, INSERM/UEVE UMR 861, Genopole Campus 1, 5 rue Henrie Desbruères, 91030 Evry cedex,[3] France

Received 31 December 2008/Returned for modification 4 March 2009/Accepted 19 March 2009

***Dppa4* (*d*evelopmental *p*luri*p*otency-*a*ssociated 4) has been identified in several high-profile screens as a gene that is expressed exclusively in pluripotent cells. It encodes a nuclear protein with an SAP-like domain and appears to be associated preferentially with transcriptionally active chromatin. Its exquisite expression pattern and results of RNA interference experiments have led to speculation that Dppa4, as well as its nearby homolog Dppa2, might play essential roles in embryonic stem (ES) cell function and/or germ cell development. To rigorously assess suggested roles, we have generated Dppa4-deficient and Dppa4/Dppa2 doubly deficient ES cells, as well as mice lacking Dppa4. Contrary to predictions, we find that Dppa4 is completely dispensable for ES cell identity and germ cell development. Instead, loss of Dppa4 in mice results in late embryonic/perinatal death and striking skeletal defects with partial penetrance. Thus, surprisingly, Dppa4-deficiency affects tissues that apparently never transcribed the gene, and at least some loss-of-function defects manifest phenotypically at an embryonic stage long after physiologic Dppa4 expression has ceased. Concomitant with targeted gene inactivation, we have introduced into the *Dppa4* locus a red fluorescent marker (tandem-dimer red fluorescent protein) that is compatible with green fluorescent proteins and allows noninvasive visualization of pluripotent cells and reprogramming events.**

Embryonic stem (ES) cells are derived from the inner cell mass of mammalian blastocysts, which is the source of all cell types of the embryo proper. In line with their developmental origin, ES cells maintain the ability to differentiate into all cell lineages of the embryonic and adult organism—a property termed pluripotency. Another key feature of ES cells is their ability to self-renew indefinitely in vitro, i.e., to proliferate continuously in an undifferentiated state under defined cell culture conditions. These unique properties have made ES cells an invaluable resource both for basic research and potential medical applications (reviewed in references 18 and 32), which in turn has triggered prime interest in the molecular mechanisms determining ES cell identity.

Despite heightened efforts in recent years, the molecular networks controlling key features of ES cells are just beginning to emerge. For murine ES cells, the Lif-gp130-Stat3-myc, Bmp4-Smad1, mitogen-activated protein kinase-extracellular signal-regulated kinase (ERK), and possibly Wnt signaling pathways are considered important extrinsic regulators of ES cell identity (reviewed in references 14, 26, 37, and 46). Signals emanating from these pathways appear to control the expression of a limited set of transcriptional regulators, which act as essential intrinsic determinants of ES cell identity. The first such intrinsic factor identified was Oct4 (36), followed by Sox2 (2), Nanog (12, 31), and most recently Ronin (16). Targeted inactivation of any member of this quartette is incompatible with maintenance of a stable pluripotent state, clearly establishing that these regulators have nonredundant roles. Importantly, three of these factors are expressed exclusively (Oct4 and Nanog) or almost exclusively (Ronin) in pluripotent cells. This observation has prompted a hunt for genes with pluripotency-associated expression patterns in anticipation of discovering additional key regulators of ES cell identity. While promising candidate genes have indeed been identified, for many of them a rigorous functional evaluation is still missing.

One gene that has come up repeatedly in several independent screens as a potential component of the genetic machinery governing key ES cell properties is *Dppa4* (*d*evelopmental *p*luri*p*otency-*a*ssociated 4). It first appeared as an ES cell-specific transcript in a comprehensive microarray profiling study (40). Shortly thereafter, it surfaced again, this time in an electronic screen designed to identify transcripts with an *Oct4*-like expression pattern (5). In an independent publication human *Dppa4* was highlighted, again as a gene that clustered closest with *Oct4*, in a comparison of expression patterns of transcripts from various cell types by microarray analysis (48). More recently, mouse *Dppa4* reemerged in an RNA interference-based functional genomics screen for genes potentially controlling self-renewal in ES cells (23). Finally, in several independent "global genome location" studies, the *Dppa4* gene locus has been traced as a prominent binding site for the core pluripotency factors Oct4, Sox2, and Nanog (3, 7, 11), which

* Corresponding author. Mailing address: Albert Einstein Allee 11, D-89081 Ulm, Germany. Phone: 49 731 5006 5210. Fax: 49 731 5006 5211. E-mail: joerg.fehling@uni-ulm.de.

† Supplemental material for this article may be found at http://mcb.asm.org/.

▽ Published ahead of print on 30 March 2009.

has been interpreted as suggesting an important role in the transcriptional circuitry controlling ES cell identity.

In sharp contrast to its accentuated appearance in multiple autonomous screens for pluripotency-associated genes, experimental data addressing the actual physiological function of Dppa4 are surprisingly scarce. Using reverse transcription-PCR (RT-PCR), whole-mount in situ hybridization, and immunocytochemistry, Maldonado-Saldivia and colleagues have characterized in meticulous detail the expression patterns of both *Dppa4* and its closest homolog, *Dppa2*, in various cell lines and during mouse development (28). The presented data firmly establish exclusive expression of both genes in pluripotent cells, i.e., only in cells of the preimplantation embryo, in ES/embryonic carcinoma cells, and cells of the developing germ line, but the data do not yield any insight into Dppa4 function. Inspection of the Dppa4 protein sequence provides only limited functional information. The open reading frame encodes a full-length protein of 296 amino acids with a single discernible protein motif, the SAP domain, named after the three proteins SAF (scaffold attachment factor), acinus, and PIAS (protein inhibitor of activated STATs) in which it was first identified (1). SAP domains encompass ~35 amino acids, which are predicted to form two amphipatic helices with DNA or RNA binding activity. The distribution of SAP domains among proteins with some known functions has suggested potential roles in chromatin organization, transcriptional gene regulation, or RNA processing, but available experimental evidence does not permit more precise predictions with regard to the specific function of the SAP domain in Dppa4. Broadly compatible with some of the suggested SAP domain activities is a recent study with ES cells that has provided biochemical and immunocytochemical evidence for preferential association of Dppa4 protein with transcriptionally active chromatin (29). Importantly, in the same study, which is so far the only one addressing specifically Dppa4 function, results of a limited set of RNA interference (RNAi) experiments were interpreted as evidence to conclude that Dppa4 is required for maintaining ES cells in an undifferentiated state (29).

To rigorously assess suggested roles of Dppa4 in ES cell function and to obtain first clues about its in vivo role, we have generated ES cell lines and mice constitutively lacking Dppa4. In contrast to predictions from expression studies and the aforementioned RNAi experiments, we demonstrate conclusively that Dppa4 is completely dispensable for maintenance of ES cell pluripotency and self-renewal and that it is also not required for germ cell development. Instead, in homozygous mutant mice derived from heterozygous parents, lack of Dppa4 results in skeletal defects and late embryonic/perinatal death, indicating an essential role during the pluripotent stage of development, which, however, appears to manifest phenotypically only long after *Dppa4* expression has ceased.

MATERIALS AND METHODS

ES cell culture. ES cells were cultured on irradiated Neo-resistant mouse embryonic fibroblasts (MEFs) in Dulbecco's modified Eagle's medium (DMEM)-Glutamax-high glucose (Gibco) medium with 15% fetal calf serum (FCS), 1 mM sodium pyruvate supplemented with nonessential amino acids (Gibco), 150 μM monothioglycerol (Sigma), and 1,000 U/ml leukemia inhibitory factor (LIF; Chemicon). For in vitro differentiation, ES cells were passaged twice in the presence of 1,000 U/ml LIF on gelatinized petri dishes to remove feeder cells. For generation of embryoid bodies, ES cells were trypsinized and plated at two different densities (30,000 cells/well for days 1 to 3 and 2,000 cells/well for days 4 to 7) in low-attachment six-well clusters (Costar) in Iscove's modified Dulbecco's medium supplemented with 15% FCS, 2 mM L-glutamine, and 450 μM monothioglycerol. For flow cytometric analysis the embryoid bodies were harvested and dissociated by trypsinization. Cells were analyzed on a FACSCalibur instrument using CellQuest software (BD Biosciences).

Generation of Dppa4-deficient and Dppa2/Dppa4 doubly deficient ES cell lines. Relevant DNA fragments of the mouse *Dppa4* and *Dppa2* gene loci were cloned from genomic DNA of line E14.1 (129/Ola-derived) ES cells by PCR using the Expand Long Template PCR System (Roche Diagnostics). The complete nucleotide sequence of the final targeting vectors for each Dppa4 allele (pVM-FF, targeting construct A; pVM-CB, targeting construct B) and of the final targeting construct for both *Dppa2* alleles (pNJ-EE, targeting construct C) can be obtained from the authors upon request. LoxP- and Flp recognition target (FRT)-flanked selection cassettes and sequences were excised by transient transfection of targeted ES cells with pCAGGS expression vectors containing an internal ribosome entry site-green fluorescent protein (GFP) cassette preceded by cDNA encoding improved Cre recombinase (45) or enhanced Flp recombinase(8), respectively. Transfected ES cells were plated on irradiated MEFs and cultured for 18 to 24 h to allow for expression of GFP. ES cells exhibiting green fluorescence were sorted by fluorescence-activated cell sorting to enrich for improved Cre recombinase- and enhanced Flp recombinase-expressing cells. Sorted cells were plated at clonal density on irradiated MEFs and cultured for 7 to 10 days until the appearance of discrete colonies. Colonies were randomly picked and plated with or without selection. Individual colonies sensitive to G418 were expanded for molecular analysis. All genetic manipulations were performed in ES cells of the E14.1 line (25).

Generation of Dppa4-deficient mice. ES cells of the E14.1 line were targeted with tandem-dimer red fluorescent protein (tdRFP)-containing construct B (plasmid pVM-CB) following established protocols (27). G418-resistant colonies were screened for correct homologous recombination by PCR using the forward primer 5′-GGTCTCAGCTCCAAACTTTGTAACTTC-3′ (complementary to sequences in intron 1 of the Dppa4 gene) and the reverse primer 5′-CCTGAA AACTTTGCCCCCTCCATA-3′ (complementary to a linker sequence flanking the Neo selection cassette). The frequency of PCR-positive clones was 5/2,496 (targeting efficiency, ~1/500 G418-resistant colonies). Independently targeted clones 167 and 842 were randomly chosen for the generation of knockout mouse lines. In clone 167, the *loxP*-flanked Neo selection cassette was excised in vitro, as described above. Heterozygous Dppa4-deficient mice were generated following classical methodology (injection of targeted ES cells into C57BL/6 blastocysts, implantation of injected blastocysts into pseudo-pregnant females, and backcross of chimeras with C57BL/6 partners). In line 842, the *loxP*-flanked Neo cassette was removed by intercrossing heterozygous animals with partners of the ubiquitous deleter strain CMV-Cre (where CMV is cytomegalovirus) (44), which had been back-crossed onto C57BL/6 for at least 12 generations. Heterozygous Dppa4-deficient animals of both independent lines were continuously backcrossed onto C57BL/6 mice. Unless stated otherwise, all data presented were obtained with animals of the fifth backcross generation.

Southern blotting. To verify correct genetic modification of Dppa4 loci, genomic DNA was isolated from targeted ES cells or mouse tail biopsy samples digested with BglII or BglII/XhoI as appropriate, blotted to nylon membrane, and hybridized with a probe located outside the targeting construct. The probe (706 bp) was obtained by PCR amplification using genomic ES cell DNA as a template and the following primer combination: 5′-CTGGAGACAAGAAGGT GAGAAC-3′ and 5′-TGGAAGTGACAATTTAGCATTTCC-3′.

RT-PCR analysis. Total RNA was extracted from ES cells using an RNeasy minikit (Qiagen) and reverse transcribed with Superscript III (Invitrogen). Dppa4 transcripts were amplified with primers annealing to sequences encoded by exons 1 and 7 (5′-ATGGAGACTGCTGGAGACAAGAAG-3′ and 5′-TCC TTCGAGGCTCTTAGTCAAGAT-3′) or by exons 3 and 6 (5′-GACACTGAG ACGCCAGGACAGACTC-3′ and 5′-TGGGGGTGGAAATGTGCAGGCC-3′) as appropriate. Dppa2 transcripts were amplified with primers 5′-ATGTCA TACTTCGGCCTGGAGAC-3′ and 5′-GGACCCTGCTTCATTCTGGCCTC-3′, which anneal to sequences encoded by exons 1 and 5, respectively.

Sequence analysis of transcripts lacking exon 2. Total RNA from Dppa4$^{-/-}$ ES clones 243.12 and 248.28 was reverse transcribed and amplified using primers 5′-TGGGGGTGGAAATGTGCAGGCC-3′ and 5′-TGGCCTTTGCTGCTCA CTCGTTTC-3′. Amplified DNA was subcloned into the pCRII-TOPO vector (Invitrogen) according to the manufacturer's instructions. Inserts were sequenced using the following primers: 11102, 5′-GTAAAACGACGGCCAGT-3′; 14013, 5′-GGAAACAGCTATGACCATGATTA-3′; BM-61, 5′-TGGCCTTTG CTGCTCACTCGTTTC-3′; and VM-37, 5′-TGGGGGTGGAAATGTGCAGG CC-3′.

Generation of polyclonal rabbit anti-Dppa4 and anti-Dppa2 sera. Polyclonal antisera were raised against peptide epitopes encoded by exon 5 (amino acids 137 to 150, TAHKKMKTEPGEES) of murine Dppa4 and exon 7 (amino acids 287 to 301, RSRAKKNALPPNMPP) of murine Dppa2. Peptide synthesis, coupling of peptides to either *Limulus* hemocyanine (for Dppa4) or keyhole limpet hemocyanin (for Dppa2) as a carrier, immunization of rabbits, and affinity purification of specific immunoglobulin Gs (IgGs) was done at Biogenes GmbH, Berlin, Germany (Dppa4), and at Eurogentec, Belgium (Dppa2).

Immunoblot analysis. ES cells grown to confluence in 10-cm-diameter petri dishes were lysed using radioimmunoprecipitation assay buffer (50 mM Tris-HCl, 150 mM NaCl, 1% Noniodet P-40, 0.5% sodium deoxycholate, 0.1% sodium dodecyl sulfate, and protease inhibitor mixture). To extract proteins, the lysate was incubated on ice for 20 min, followed by centrifugation at 14,000 × *g*. The amount of total protein extracted was estimated using Bradford's reagent (Bio-Rad). Equal amounts of proteins were resolved on 10% sodium dodecyl sulfate-polyacrylamide gels and then blotted onto Immobilon-P membranes (Millipore). After being blocked with blotting grade milk (3% in phosphate-buffered saline [PBS]), the membranes were incubated with primary antibody (anti-Oct4 at 1/500 [Santa Cruz Biotechnology Inc.], anti-Nanog at 1/5,000 [Bethyl Laboratories], anti-Sox2 at 1/2,000 [Chemicon International], and affinity-purified anti-Dppa4 serum at 1/100 or anti-Dppa2 serum at 1/200) overnight at 4°C. Unbound primary antibody was removed by washing with 0.1% Tween 20 in PBS. The membrane was then incubated with horseradish peroxidase-conjugated anti-rabbit IgG antibody (1/10,000). Following several washes, the blot was developed using enhanced chemiluminescence reagent (SuperSignal West Dura Extended Duration Substrate; Pierce). Blotting with anti-ERK antibody (1/1,000; Santa Cruz Biotechnology Inc.) was used to verify equal loading of protein lysates.

AP staining. ES cells were stained using an alkaline phosphatase (AP) detection kit (Chemicon) following the manufacturer's instruction. Briefly, ES cells were plated at low density on irradiated feeders. After 5 days the colonies were fixed with 90% methanol–10% formaldehyde. Following fixation, colonies were rinsed with buffer (20 mM Tris-HCl, pH 7.4, 150 mM NaCl, 0.05% Tween-20) and stained with AP staining solution for 15 min at room temperature. The cells were rinsed with rinse buffer and covered with PBS to prevent drying. Genital ridges were dissected from embryos at day 12.5 of gestation (E12.5) and fixed with 4% paraformaldehyde in PBS for 2 h at 4°C. Following washes with PBS, genital ridges were incubated with 70% ethanol for 1 h at 4°C. To remove excess ethanol, the genital ridges were washed with water and then stained with Naphthol-FastRed solution for 15 min at room temperature as described previously (20). The preparations were cleared and mounted in 70% glycerol.

Self-renewal competition assay (23). Homozygous Dppa4-deficient ES cells (RFP positive) and wild-type ES cells (RFP negative) were mixed at three different ratios (3:1, 1:1, and 1:3), and a total of 1 $\times 10^6$ cells were plated on irradiated MEF feeder layers in 10-cm-diameter petri dishes. Cells were harvested after 48 h and analyzed by flow cytometry for the ratio of RFP-positive to RFP-negative cells. An aliquot of harvested cells was replated at the same density as before, and the same procedure was followed for seven passages.

Generation and analysis of chimeric mice to assess ES cell pluripotency. To monitor the in vivo developmental potential of mutant ES cells, Dppa4$^{-/-}$ cells of clone 248.44 and of a subclone of 243.12 (carrying a targeted *lacZ* reporter in one ROSA26 allele) were injected into BALB/c blastocysts, which were subsequently implanted into pseudo-pregnant females. Chimeric animals were analyzed either as E18.5 embryos or as young adults (5 to 10 weeks old) using immunohistochemistry, flow cytometry, *lacZ* staining and PCR techniques.

Immunofluorescence studies were performed on acetone-fixed 5-μm-thick cryosections. Endogenous biotin activity was blocked using a biotin blocking kit (Invitrogen), followed by incubation with anti-mouse CD16/CD32 (BD Pharmingen) to block nonspecific binding of antibodies. The sections were then incubated with Phycoerythrin (PE)-labeled H-2K^b and/or biotinylated H-2K^d antibodies (BD Pharmingen). Following removal of unbound antibody, sections were incubated with AlexaFluor-647-conjugated streptavidin (Molecular Probes, Carlsbad, CA), and nuclei were counterstained with 4′,6′-diamidino-2-phenylindole (DAPI) and mounted with Fluoromount-G. The staining was examined under a fluorescence microscope (Axioscop; Zeiss).

For β-galactosidase staining, 10- to 15-μm-thick cryosections were fixed with 0.125% glutaraldehyde and 2% paraformaldehyde in PBS for 5 min at room temperature. The fixed sections were washed with PBS containing 2 mM $MgCl_2$ and then incubated with X-Gal (5-bromo-4-chloro-3-indolyl-β-D-galactopyranoside; 1 mg/ml in reaction buffer containing 30 mM potassium ferricyanide, 30 mM potassium ferrocyanide, 2 mM magnesium chloride, 0.01% sodium deoxycholate, 0.02% NP-40 in PBS) at 37°C overnight. The slides were then rinsed with PBS containing 2 mM $MgCl_2$ and mounted in glycerol-gelatin (Sigma).

For flow cytometric analysis of lymphocyte populations, single-cell suspensions were prepared from lymph nodes of chimeric and age-matched control mice. Fc receptors were blocked with anti-CD16/CD32 antibody (BD Pharmingen) for 15 min on ice. For each staining 1 × 10^6 cells were incubated with appropriate antibodies in 50 μl of PBS containing 5% FCS. Primary antibodies used were PE-labeled-CD3 or PE-labeled CD19, biotinylated-H-2K^b, and fluorescein isothiocyanate-labeled H-2D^d (all BD Pharmingen). Second-step reagent was streptavidin-allophycocyanin (Molecular Probes, Carlsbad, CA). Stained cells were analyzed on a FACSCalibur using CellQuest software (BD Biosciences).

DNA chimerism was quantified by PCR using genomic DNA from various organs of chimeric mice as a template. Dppa4 wild-type and knockout alleles were specifically amplified in a single reaction with the forward primer BM-79 (5′-TGGCTGCCCTGGAACTCACTCT-3′) and reverse primers BM-80 (5′-CTTGTCTCAACACCGCCCACC-3′; wild-type-specific primer, complementary to sequences in intron 1 and intron 2, respectively) and HL-51 (5′-CCTGAAAACTTTGCCCCCTCCATA-3′; knockout-specific primer, complementary to linker sequences in the Neo selection cassette).

Subcellular distribution studies with GFP fusion constructs. cDNA encoding full-length Dppa4 or its natural splice variant (lacking the SAP domain) was obtained by RT-PCR. Total RNA extracted from E14.1 ES cells was reverse transcribed and amplified with primer combination 5′-ATGGAGACTGCTGGAGACAAGAAG-3′ and 5′-TCCTTCGAGGCTCTTAGTCAAGATC-3′ using an Expand Long Template PCR system (Roche). PCR fragments of predicted length were cloned into pCRII-TOPO vector and verified for the correct nucleotide sequence by dideoxy sequencing. Full-length Dppa4 and its splice variant were then cloned into the unique EcoRI site of expression vector pEGFP.C2 (Clontech). This cloning results in an open reading frame encoding enhanced GFP (EGFP) under the control of the CMV promoter fused in-frame to Dppa4 or its splice variant, respectively.

To visualize cellular localization of GFP-Dppa4 proteins, fusion constructs or pEGFP.C2 as a control were transiently transfected into human pancreatic carcinoma cells (Panc-1), which were maintained in DMEM supplemented with 10% FCS and antibiotics. One day prior to transfection, 6 × 10^4 cells were plated on 12-mm-diameter sterile coverslips placed in 24-well plates. Liposome-mediated DNA transfection was carried out using DIMRIE-C (1,2-dimyristyloxypropyl-3-dimethyl-hydroxy ethyl ammonium bromide and cholesterol) reagent (Invitrogen) according to the manufacturer's protocol. At 24 h after transfection, the cells were fixed with 2% paraformaldehyde (pH 7.2) and rinsed with methanol, and nuclei were stained with DAPI. Coverslips were subsequently mounted in Fluoromount-G. Green fluorescence was monitored under a microscope (Axioscop; Zeiss), and images were analyzed using OpenLab software.

Microarray analysis. For expression profiling 1 μg of total RNA was linearly amplified and biotinylated using a One-Cycle Target Labeling Kit (Affymetrix, Santa Clara, CA) according to the manufacturer's instructions. Fifteen micrograms of labeled and fragmented cRNA was hybridized to MOE430 2.0 Gene Chip arrays (Affymetrix). After hybridization the arrays were washed and stained in a Fluidics Station 450 (Affymetrix) with the recommended washing procedure. Biotinylated cRNA bound to target molecules was detected with streptavidin-coupled PE, biotinylated anti-streptavidin IgG antibodies, and again streptavidin-coupled PE according to the protocol. Arrays were scanned using the GCS3000 GeneChip scanner (Affymetrix) and GeneChip Operating Software, version 1.4. Scanned images were subjected to visual inspection to control for hybridization artifacts and proper grid alignment and analyzed with Microarray Suite, version 5.0 (Affymetrix), to generate report files for quality control. For statistical data assessment CEL files were analyzed on the software platform R (version 2.7.0) using the bioconductor packages affy and limma. Background correction, normalization, and probe summarization were performed with robust multichip average analysis yielding log2-transformed signal values for all arrays. Additionally, detection calls were created using the MAS5 algorithm. Transcripts that were called "absent" in all six arrays were excluded from further analysis. For the remaining transcripts, a linear model was calculated whose coefficients describe the observed expression profiles. Differentially expressed transcripts between cell lines were extracted using a moderated *t* test (empirical Bayes method) including a correction step for multiple testing (4, 47). Annotations for the differentially expressed transcripts were extracted from the bioconductor package mouse4302.db and subjected to overrepresentation analysis at the Panther (protein analysis through evolutionary relationships) website (http://www.pantherdb.org).

Quantitative real-time PCR validation of microarray data. Relative expression of selected mRNA targets was determined by quantitative real-time PCR. Five hundred nanograms of total RNA was reverse transcribed using a QuantiTect Reverse Transcription Kit (Qiagen, Hilden, Germany) according to manufacturer's instruction. cDNA was diluted 1:10 prior to PCR amplification. Primers were designed with Primer3 (http://www-genome.wi.mit.edu/cgi-bin/primer

/primer3_www.cgi) and synthesized by Metabion (Martinsried, Germany). A list of PCR targets and primers is available on request. Real-time detection of specific PCR products was performed on a LightCycler480 (Roche, Penzberg, Germany) with 5 μl of 2× QuantiTect SYBR green PCR kit solution (Qiagen, Hilden, Germany), a 300 nM concentration of each forward and reverse primer, 2 μl of diluted cDNA, and aqua bidest to a final volume of 10 μl. PCR was initiated by a 10-min hot start, followed by 45 cycles of 95°C for 20 s, 58°C for 40 s, and 72°C for 20 s. Fluorescence was measured at the end of the elongation step. Amplification of specific PCR products was checked in a subsequent melting curve analysis. Each PCR was performed in three technical replicates; PCR efficiency was calculated from fourfold serial dilutions of an equal mixture of all cDNAs using the following equation: $E = 10^{-1/\text{slope}}$ (42). To calculate the relative expression of each target, the raw crossing point values were imported into qBASE (22). Three suitable reference genes (TBP, PDHB, and YWHAZ) were selected according to their gene stability values and used for normalization of the quantitative real-time PCRs (21).

Preparation of tissues for histological examination. Lungs were taken from surviving newborns or E18.5 embryos within a few hours after birth or after Caesarian delivery, respectively. Tissues were fixed in 4% paraformaldehyde, pH 7.4 (lungs), or Bouin's solution (testes and ovaries) (Sigma) overnight at 4°C. After excess fixative was removed, tissues were washed through ethanol gradients to dehydrate, cleared with xylene, embedded in paraffin, and stored at 4°C. Sections (5 μm) were cut from paraffin blocks using a microtome (RM2255; Leica Microsystems). The sections were spread in a water bath at 37°C and transferred to SuperFrost Plus slides (catalog no. J1800AMNZ; Menzel GmbH, Braunschweig, Germany). The sections were allowed to spread overnight in a 37°C oven and were then stored at room temperature. For hematoxylin-eosin (H&E) staining, paraffin sections were dewaxed using xylene and rehydrated through graded concentrations of ethanol. The sections were rinsed in distilled water, and nuclei were stained with hematoxylin (Merck) for 5 to 8 min. After the slides were washed with water for 10 min, the cytoplasm was counterstained with 0.25% eosin (Sigma) for 3 min. The slides were washed briefly with distilled water, dehydrated with increasing concentrations of ethanol, cleared in xylene, and mounted with Vectashield (Vector Laboratories Inc.). The stained sections were photographed using a DP11 camera from Olympus.

Whole-mount skeletal preparation. Mouse E18.5 embryos were delivered by Caesarean section. The skin of the embryo was removed by brief incubation in PBS at 65°C, followed by fixation of the embryos in 100% ethanol overnight. The cartilage was stained by incubating the embryos for 2 days in ethanol containing 5% acetic acid and 150 mg/liter alcian blue 8GX. To remove excess dye, specimens were washed for 3 days in ethanol and subsequently cleared in 2% KOH for 1 to 2 h. Once the embryos were translucent and staining of the cartilage was visible, ossified skeleton was stained by overnight incubation in 0.5% KOH containing 50 mg/liter alizarin red S, followed by clearing in 1% KOH. Skeletal preparations were stored in 40% glycerol at 4°C.

PI staining and flow cytometry of sperm from adult males. Testis were decapsulated, and tubules were minced in collagenase A solution (0.4 mg/ml in PBS). Following incubation for 45 min at room temperature with gentle mixing, the cell slurry was passed through a 100-μm-pore-size cell strainer (BD). Cells were collected by centrifugation at 1,000 rpm for 5 min at 4°C, washed with PBS, and resuspended in 2 ml of 70% ethanol. After incubation at 4°C for 45 min with gentle mixing, cells were pelleted as above and washed once with PBS. Cells were incubated in 1 ml of propidium iodide (PI) buffer (15 μg/ml PI, 0.25% NP-40, and 50 μg/ml RNase A in PBS) for 20 min at room temperature protected from light. Samples were acquired on a FACSCalibur instrument and analyzed using Cell Quest software (BD Biosciences).

Flow cytometric analysis of primordial germ cells. Genital ridges were dissected from E12.5 embryos. To dissociate the cells, genital ridges were incubated with 0.05% trypsin-EDTA (Gibco) for 5 min at 37°C. The resulting single-cell suspensions were washed with PBS, and cells were stained with allophycocyanin-labeled anti-mouse CD117 (anti-mouse Kit) antibody (BD Pharmingen). Stained cells were analyzed on a FACSCalibur instrument using CellQuest software (BD Biosciences).

Fluorescence microscopy. Genital ridges and newborn testes were examined under a fluorescence stereomicroscope (Leica MZ16F) equipped with external light source and appropriate filter sets (excitation filter, 545 ± 15 nm; emission filter, 620 ± 30-nm band-pass filter; Leica, Heerbrugg, Switzerland). Fluorescent imaging of ES cells and preimplantation embryos was performed with the inverse fluorescence microscope Axiovert 25 (Carl Zeiss) equipped with appropriate filter sets (excitation filter, 565 ± 30 nm; emission, 620 ± 60-nm band-pass filter; Zeiss).

Reprogramming of tdRFP/Dppa4 knock-in MEFs. MEFs were isolated from genotyped embryos (E14.5) of heterozygous tdRFP/Dppa4 knock-in parents. The day before infection, each embryonic fibroblast population was seeded at 10^5 cells per well in six-well plates. Twenty-four hours later, cells were infected with a mix of three retroviruses encoding human OCT4, SOX2, and KLF4, respectively (produced by Vectalys, Labège, France), in normal medium supplemented with 8 μg/ml polybrene (Sigma) following established protocols (34). On day 3, cells were trypsinized and plated on a feeder layer (20,000 feeders/cm^2) in 10-cm gelatinized petri dishes. Medium was changed every 2 to 3 days, and on day 7 it was replaced with mouse ES cell-specific medium containing knockout DMEM, 15% knockout serum replacement, 1× nonessential amino acids, 2 mM glutamine, 100 units/ml penicillin, 100 μg/ml streptomycin (all products from Gibco), and LIF (generous gift from Mouse Clinical Institute, Strasbourg, France). RFP-positive clones were picked between 3 and 4 weeks postinfection, amplified in the same medium, and frozen with 10% dimethyl sulfoxide (Sigma). Photographs were taken using a CoolSNAP camera (Roper Scientific, Evry, France) on a Leica DMIRE2 microscope (Rueil-Malmaison, France) and analyzed with Metamorph software (MDS Analytical Technologies, Concord, Canada). Phase-contrast and fluorescent pictures were taken with an exposure time of 10 ms and 1,000 ms, respectively.

Microarray data accession number. All reported microarray data have been deposited in the public database Gene Expression Omnibus (http://www.ncbi.nlm.nih.gov/projects/geo) under accession number GSE 15173.

RESULTS

Generation of homozygous Dppa4-deficient ES cells and insertion of a red fluorescent reporter gene into the Dppa4 gene locus. To explore potential functions of Dppa4 in pluripotent cells, we have generated Dppa4-deficient mouse ES cells via sequential gene targeting and Cre-*loxP*-mediated recombination. Homozygous inactivation of a critical pluripotency gene might lead to rapid loss of ES cell identity and thus preclude identification of mutant clones. We therefore followed a strategy in which only one allele of Dppa4 was constitutively inactivated while the other was modified by insertion of *loxP* sites to allow conditional inactivation through Cre-mediated recombination. Using targeting construct A (Fig. 1A, top left), *loxP* sites were introduced into intronic sequences upstream and downstream of exon 2. Two correctly targeted ES clones (84 and 180) (Fig. 1B) were identified. The FRT-flanked Neo resistance cassette cointroduced into the locus during gene targeting was removed in both clones by in vitro Flp-mediated recombination, giving rise to several Neo-sensitive subclones, of which two (84.2 and 180.5) (Fig. 1B) were randomly picked for characterization of the modified locus and targeting of the second *Dppa4* allele. In a subsequent round of gene targeting experiments, we introduced construct B (Fig. 1A, top right) into ES cells of both independent clones 84.2 and 180.5 and successfully generated subclones 243 and 248 (derived from 84.2 and 180.5, respectively) (Fig. 1B), in which exon 2 on the second *Dppa4* allele was replaced with a stretch of foreign DNA consisting of a splice acceptor site (SA), a cDNA encoding tdRFP, followed by an simian virus 40 polyadenylation signal (pA), and finally a *loxP*-flanked Neo resistance gene (Fig. 1A, top right). tdRFP is a very bright RFP (9) that has recently been demonstrated to provide a convenient, nontoxic marker for noninvasive monitoring of gene expression in ES cells and gene-targeted mice (27). Insertion of the SA-tdRFP-pA cassette in lieu of exon 2 is expected to capture and truncate the *Dppa4* transcript after the first 8 codons, thus giving rise to a novel message that encodes full-length tdRFP fused to a few additional amino acids at its N terminus.

For generation of homozygous Dppa4-deficient ES cells from heterozygous mutants, we chose a strategy that would unmask any significant loss of ES cell identity during the pro-

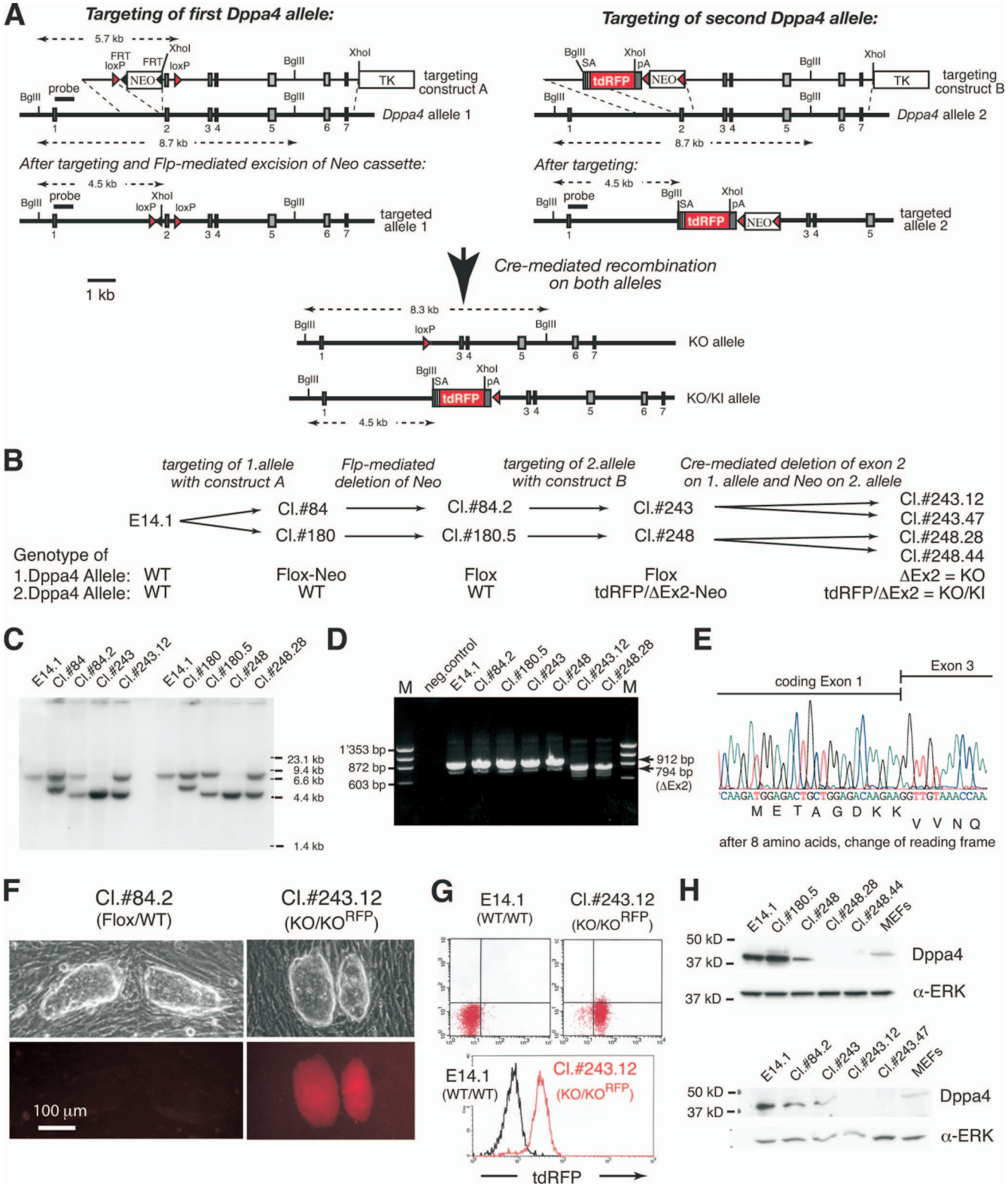

FIG. 1. Homozygous inactivation of *Dppa4* in ES cells and concomitant insertion of a red fluorescent reporter gene into one *Dppa4* allele (*Dppa4*^{tdRFP}) by successive gene targeting. (A) Targeting strategy used to generate homozygous Dppa4-deficient ES cells with one *Dppa4*^{tdRFP} knock-in (KI) allele. Filled boxes, exons; red triangles, *loxP* sites; black triangles, FRT sites; TK, thymidine kinase cassette for selection against random integration events. (B) Targeting history of individual Dppa4-modified ES clones. Flox-Neo, allele on which exon 2 has been flanked by *loxP* sites (floxed) and a FRT-flanked Neo selection cassette inserted into intronic sequences upstream of exon 2; Flox, allele on which *Dppa4* exon 2 has been flanked by *loxP* sites; tdRFP/ΔEx2-Neo, allele on which *Dppa4* exon 2 has been replaced by a tdRFP expression cassette and a *loxP*-flanked Neo cassette; tdRFP/ΔEx2, allele on which *Dppa4* exon 2 has been replaced by the tdRFP expression cassette; ΔEx2, allele on

cess of complete Dppa4 gene inactivation. Briefly, ES cells of heterozygous Dppa4-deficient clones 243 and 248 were electroporated with an expression vector (pCre-AC) encoding a Cre recombinase-internal ribosome entry site-GFP cassette. Approximately 24 h later, Cre recombinase-expressing ES cells were identified by flow cytometry based on GFP expression; cells were sorted and plated at clonal density on irradiated MEFs. After 8 days of in vitro culture, ES colonies were counted and individually analyzed for Cre-mediated loss of G418 resistance and excision of exon 2 on the floxed *Dppa4* allele. A total of 80/96 colonies (~83%) derived from clone 243 and 74/88 colonies (~84%) from clone 248 had undergone Cre-mediated recombination. Neither the number of surviving colonies after GFP-based sorting nor the frequency of recombined clones was different from previous experiments, in which nonessential genes (like the Neo cassette) had been deleted following the same strategy. These observations demonstrate that homozygous inactivation of Dppa4 can be achieved at high frequency in pluripotent embryonic stem cells and that successful identification of Dppa4-deficient ES colonies is not due to outgrowth of rare mutant cells selected for compensation of Dppa4 deficiency.

For further analysis, two homozygous Dppa4-deficient subclones were randomly selected from recombined progeny of each of the "ancestor" clones 243 and 248 (Fig. 1B). All genetic modifications were confirmed on genomic DNA by PCR with appropriate primers (data not shown) and by Southern blotting with a probe located outside of both targeting constructs (Fig. 1C). RT-PCR analysis of *Dppa4* transcripts with primers complementary to sequences in the first and last exon revealed the expected pattern of amplified fragments in all clones analyzed. As anticipated, insertion of *loxP* sites (clones 84.2 and 180.5) had no detectable influence on transcript size, while Cre-mediated deletion of exon 2 (clones 243.12 and 248.28) resulted in correspondingly smaller transcripts (Fig. 1D). Sequence analysis of truncated message confirmed the absence of exon 2-encoded sequences, correct splicing between newly juxtaposed exons 1 and 3, and, importantly, the predicted disruption of the *Dppa4* reading frame after just eight N-terminal amino acids (Fig. 1E). As insertion of the SA-tdRFP-pA expression cassette on the second *Dppa4* allele is expected to prevent transcription beyond the pA, we were unable to detect any wild-type message in homozygously targeted ES cells (Fig. 1D, clones 243.12 and 248.28). In line with our prediction, all ES clones in which exon 2 had been replaced by the tdRFP cassette exhibited red fluorescence, as documented by fluorescence microscopy (Fig. 1F) and flow cytometry (Fig. 1G). Finally, we raised a polyclonal rabbit antiserum against an epitope encoded by exon 5 of mouse *Dppa4*, i.e., outside of the deleted region. Immunoblotting of cell extracts from various ES clones with wild-type and modified Dppa4 gene loci confirmed the specificity of our serum and revealed a complete absence of Dppa4 at the protein level in ES cells with homozygously disrupted *Dppa4* genes (Fig. 1H).

ES cell morphology and expression of critical pluripotency marker genes is fully maintained in the absence of Dppa4. ES cells with inactivated *Dppa4* on one or both alleles were morphologically indistinguishable from wild-type ES cells and could be continuously propagated under nondifferentiating culture conditions without any obvious phenotypic changes. To further characterize Dppa4-deficient ES cells, we assayed for expression of tissue-nonspecific AP (TNAP), an enzyme widely used as indicator for undifferentiated cells (20). ES colonies of all three Dppa4 genotypes (+/+, +/−, and −/−) stained homogenously and indistinguishably (Fig. 2A), indicating maintenance of an undifferentiated phenotype even in the absence of Dppa4. Finally, immunoblotting of cell extracts from Dppa4-deficient ES cells and appropriate controls revealed unaltered protein expression of key regulators of pluripotency, like Sox2 (2), Oct4 (36), and Nanog (12, 31) (Fig. 2B). Taken together, these findings indicate that *Dppa4* expression is not required for maintenance of an undifferentiated ES cell phenotype.

Efficient self-renewal of ES cells lacking Dppa4. Ivanova and colleagues (23) reported a sensitive fluorescence-based competition assay, which permitted a systematic search for genes involved in ES cell self-renewal. ES cells were transduced with lentiviral vectors expressing inhibitory short hairpin RNA (shRNA) against selected target genes along with GFP. GFP-positive, shRNA-transduced ES cells were mixed at a fixed ratio with nontransduced, GFP-negative cells and cultured for several passages under nondifferentiating conditions. A reduction in the GFP-positive/GFP-negative cell ratio was shown to be a sensitive indicator for compromised self-renewal in the presence of a given shRNA. Interestingly, progressive decreases in the GFP-positive/GFP-negative cell ratios were observed upon downregulation of 10 genes, including the known pluripotency genes *Oct4*, *Sox2*, and *Nanog* and, notably, *Dppa4*. Although further analyses could not provide additional evidence for an essential role of Dppa4 in self-renewal—in con-

which *Dppa4* exon 2 has been deleted. (C) Southern blot analysis of targeted ES clones described in panel B. Genomic DNA was doubly digested with BglII/XhoI and probed with a DNA fragment hybridizing downstream of exon 1 but outside the targeting construct. (D) RT-PCR analysis of total RNA from ES cells of the indicated clones with primers annealing to sequences encoded by the first and last *Dppa4* exons (exon 1 and 7). The PCR product of 912 bp represents full-length *Dppa4* message, while the product of 794 bp reveals absence of exon 2 and efficient splicing from exon 1 to exon 3 on the ΔEx2 allele. Note that insertion of the tdRFP expression cassette along with pA on the second *Dppa4* allele blocks transcription beyond the insertion site and thus does not give rise to any PCR product with the specific primers used. (E) Sequence analysis of the splice junction in the 794-bp RT-PCR fragment shown in panel D. The nucleotide sequence confirms splicing between exon 1 and exon 3 on the *Dppa4* knockout (KO) allele and the resultant shift in the reading frame, which leads to the appearance of an in-frame stop codon (TGA) after 33 amino acids (not shown). (F) Phase-contrast (top) and fluorescence (bottom) microscopy demonstrating that insertion of a tdRFP expression cassette in lieu of exon 2 on one *Dppa4* allele results in specific labeling of targeted ES cells. The configuration of *Dppa4* alleles is given in brackets. (G) Flow cytometric analysis of ES cells carrying one *Dppa4*^{tdRFP} allele (clone 243.12) and a genetically unmanipulated control (E14.1). The histogram shows an overlay of the dot plots above. (H) Immunoblot of protein extracts from the indicated ES cell clones demonstrating absence of Dppa4 protein in clones carrying a KO and a KO/KI allele (clones 248.28, 248.44, 243.12, and 243.47). The polyclonal rabbit anti-mouse Dppa4 serum used is directed against an epitope encoded by exon 5. The signal in the MEFs lane is a nonspecific band of bigger size. WT, wild type.

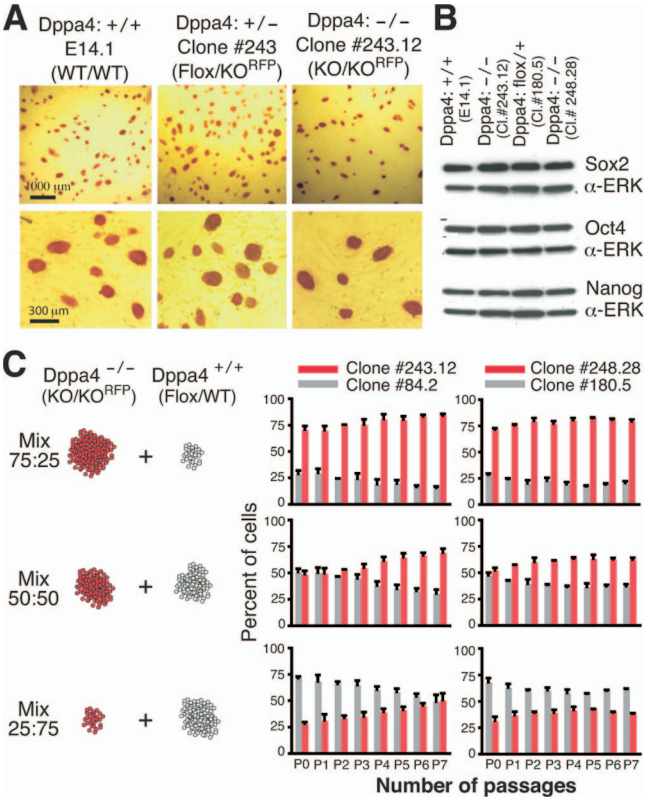

FIG. 2. Maintenance of ES cell identity in the absence of Dppa4. (A) TNAP staining of fixed ES cell colonies carrying the indicated *Dppa4* alleles. (B) Immunoblot showing expression of marker proteins (Sox2, Oct4, and Nanog) characteristic for pluripotent cells. (C) Result of sensitive fluorescence-based competition assay (23) directly comparing self-renewal ability of Dppa4-deficient ES cells with Dppa4-proficient controls. Red fluorescent, Dppa4-deficient ES cells of clone 243.12 and 248.28 were mixed at indicated ratios with appropriate $Dppa4^{Flox/+}$ ancestor ES cells (nonfluorescent) and cultured under nondifferentiating conditions. At each passage the percentage of tdRFP-positive (red bars) and tdRFP-negative (gray bars) cells was measured by flow cytometry. WT, wild type; KO, knockout; α, anti.

trast to three other newly identified candidate genes—the appearance of *Dppa4* in this unbiased screen seemed sufficiently intriguing to justify a specific scrutiny for potential self-renewal defects in constitutively Dppa4-deficient ES cell clones. Incidentally, *Dppa4*-driven tdRFP expression in our homozygous knockout clones (Fig. 1G) allowed us to apply the same fluorescence-based competition assay (23), with the advantage that we did not need to resort to retroviral transduction and shRNA-mediated suppression.

To probe the self-renewal ability of mutant versus wild-type ES cells, homozygous Dppa4-deficient, tdRFP-expressing ES cells were mixed with corresponding nonfluorescent $Dppa4^{Flox/+}$ ancestor cells at three different ratios (75:25, 50:50, and 25:75) and cultured under nondifferentiating conditions for 2 to 3 weeks. tdRFP-positive/tdRFP-negative cell ratios were measured by flow cytometry at every passage. Figure 2C shows the results for both independently derived Dppa4-deficient clones 243.12 and 248.28. Irrespective of the starting ratio, we did not observe any decrease in the number of red fluorescent cells over time. If anything, Dppa4-deficient clone 243.12 seemed to exhibit a marginally enhanced proliferative potential. These findings effectively exclude an obligatory role of Dppa4 in ES cell self-renewal.

Dppa4-deficient ES cells contribute efficiently to ectodermal, endodermal, and mesodermal tissues in chimeric mice. To assess the developmental potential of $Dppa4^{-/-}$ ES cells under in vivo conditions, we injected mutant ES cells from two independent clones (243.12 and 248.44) into wild-type BALB/c blastocysts and generated chimeric mice. The contribution of homozygous Dppa4-deficient ES cells to differentiated tissues was determined in three complementing ways. (i) Immunohistochemistry and cytofluorometry were used to exploit major histocompatibility complex (MHC) differences between ES-derived (129/Ola; $H\text{-}2^b$) and blastocyst-derived (BALB/c; $H\text{-}2^d$) tissues. (ii) *lacZ* staining was performed to detect β-galactosidase activity. As expression of MHC class I antigens is low in some cell types (e.g., nerve tissues), we had labeled one of the Dppa4-deficient ES clones (243.12) by targeting a *lacZ* gene into the ubiquitously expressed ROSA26 locus (50). (iii) Semiquantitative PCR on genomic DNA was used with oligonucleotide primers that can distinguish between Dppa4 wild-type and mutant alleles. Due to the sensitivity of the PCR, this approach was expected to detect even minor contributions of mutant ES cells to organs of chimeric mice.

Blastocyst injections resulted in a total of 19 animals, 13 of which were sacrificed and dissected as E18.5 embryos, while the remaining 6 were analyzed as young adults. All three methods to monitor chimerism provided unambiguous evidence for significant contribution of Dppa4-deficient ES cells to all organs analyzed. Representative examples are shown in Fig. 3. Importantly, our analysis revealed robust contribution of $Dppa4^{-/-}$ ES cells to tissues/cells of endodermal (Fig. 3A, liver), mesodermal (Fig. 3B), and ectodermal (Fig. 3C) origin. Contribution to differentiated tissues from all three germ layers under the controlled environment of mouse embryogenesis and in competition with blastocyst-derived wild-type cells demonstrates unequivocally that ES cells do not need Dppa4 for the maintenance of a pluripotent state.

Functional redundancy with Dppa2 cannot account for the maintenance of ES cell identity in Dppa4-deficient ES cells. Immediately downstream of the *Dppa4* gene locus resides *Dppa2*, a highly homologous gene with a very similar, if not identical, expression pattern (28). *Dppa4* and *Dppa2* are separated by just 16.8 kb of noncoding sequence, are arranged in the same transcriptional orientation, exhibit an almost superimposable exon/intron organization, and share 32% identity and 47% similarity at the amino acid level (http://www.ensembl.org/Mus_musculus/geneview?gene=ENSMUSG00000072419; http://www.ensembl.org/Mus_musculus/geneview?gene=ENSMUSG00000058550) (28), strongly suggesting that they arose by gene duplication from a common ancestor gene. As for Dppa4, no data on physiological functions of Dppa2 are yet available. To investigate whether functional redundancy between these neighboring genes might be responsible for the absence of apparent defects in ES cells lacking Dppa4, we generated Dppa2/Dppa4 doubly deficient ES cell lines by successive rounds of gene targeting. To this end, we first introduced *loxP* sites upstream and downstream of exon 2 into both *Dppa2* alleles of Dppa4-deficient clone 248.44, as outlined in Fig. 4A and B. Subsequent transient transfection with a Cre-encoding expression vector re-

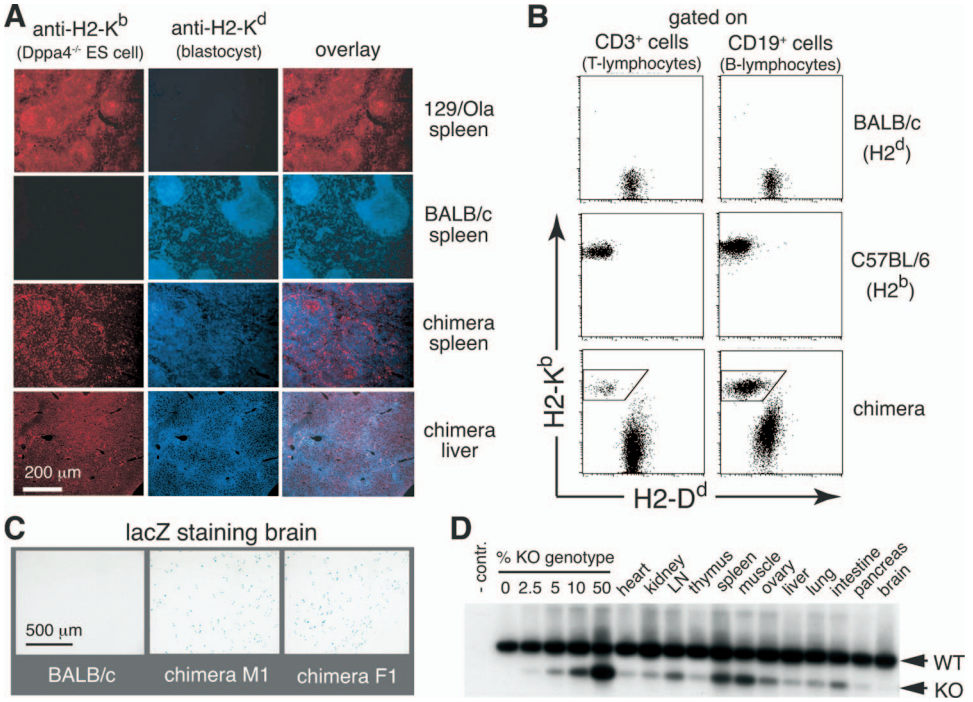

FIG. 3. Analysis of mouse chimeras generated with wild-type blastocysts from BALB/c mice (MHC, $H2^d$) and Dppa4-deficient ES cells (MHC, $H2^b$). (A) Immunohistochemistry with haplotype-specific anti-H2-K antibodies demonstrating contribution of Dppa4-deficient ES cells to spleen and endoderm-derived hepatic tissues. (B) Flow cytometric analysis of mesoderm-derived blood lymphocytes from a chimeric mouse and appropriate haplotype-controls. B and T lymphocytes originating from Dppa4-deficient ES cells are framed. (C) Dppa4-deficient ES cells carrying a β-galactosidase marker gene in the ubiquitously expressed ROSA26 locus contribute to ectoderm-derived neuronal tissues as evidenced by *lacZ* staining of fixed brain sections. (D) Analysis of tissues from a weak chimera by semiquantitative RT-PCR. Genomic DNA from the indicated organs was amplified with primers that allow distinction between *Dppa4* wild-type (WT) and knockout (KO) alleles. Titration was performed with genomic DNA from wild-type and homozygous Dppa4-deficient ES cells that had been mixed at the indicated ratios (lanes 0, 2.5, 5, 10, and 50). LN, lymph node.

sulted in straightforward generation of multiple Dppa2/Dppa4 doubly deficient clones, two of which (30.15 and 30.18) were randomly chosen for more detailed characterization.

Inactivation of *Dppa2* alleles resulted in the expected size reduction of *Dppa2* mRNA as determined by RT-PCR (Fig. 4C). Complete absence of Dppa2 protein was demonstrated with a newly generated polyclonal rabbit anti-mouse Dppa2 serum directed against an epitope encoded by exon 7 (Fig. 4D). Importantly, Dppa2/Dppa4 doubly deficient clones were homogenously positive by staining for the pluripotency marker TNAP and did not exhibit any obvious changes in ES cell morphology (Fig. 4E). Immunoblot analysis revealed wild-type protein levels for the critical pluripotency-mediating factors Sox2, Oct4, and Nanog despite combined absence of both Dppa2 and Dppa4 (Fig. 4F). Finally, homozygous inactivation of both Dppa2 and Dppa4 did not markedly alter ES cell proliferative potential or cell cycle kinetics (Fig. 4G and H). Although we did not specifically assay the developmental potential of Dppa4/Dppa2 doubly deficient ES cells, their unaltered morphology, continued expression of critical pluripotency genes, and unimpaired self-renewal ability strongly suggest that functional redundancy between Dppa4 and Dppa2 is not responsible for the maintenance of an ES cell identity in the absence of Dppa4. At the same time, our experiments demonstrate that lack of Dppa2 is fully compatible with a bona fide ES cell phenotype.

Effects of Dppa4-deficiency on the ES cell transcriptome. Dppa4 contains a SAP domain, which has been considered a putative DNA/RNA binding motif (1), and biochemical studies have provided evidence for an association of Dppa4 protein with transcriptionally active chromatin (29). Moreover, by using immunocytochemistry, the Dppa4 homolog Dppa2, which also contains an SAP domain, was shown to localize to the nucleus in cells of the preimplantation embryo (28). In line with these reports, our own immunofluorescence studies in Panc-1 cells revealed specific nuclear localization of EGFP-tagged full-length Dppa4 (Fig. 5A, middle panels). Interestingly, exclusive nuclear localization was lost when EGFP was fused to a natural, in-frame splice variant of Dppa4 lacking amino acids 81 to 115 (Val^{81}-Asn^{82} to Arg^{114}-Ala^{115}), and thus the SAP domain (Fig. 5A, right panels). Although this SAP-deficient isoform of Dppa4 can be detected by RT-PCR as a minor band in all Dppa4-positive samples (Fig. 5B to D), it appears to be expressed at particularly high levels in the testis (Fig. 5B and C). While the physiological role of this splice variant and its differential expression remain elusive, our findings strongly suggest that the SAP domain is critical for keeping Dppa4 in the nucleus. Notably, the targeting strategy we used to generate Dppa4-deficient cells (and mice[see below]) prevents expression of both isoforms.

The presence of an SAP domain, nuclear localization, and apparent association with active chromatin may indicate a role

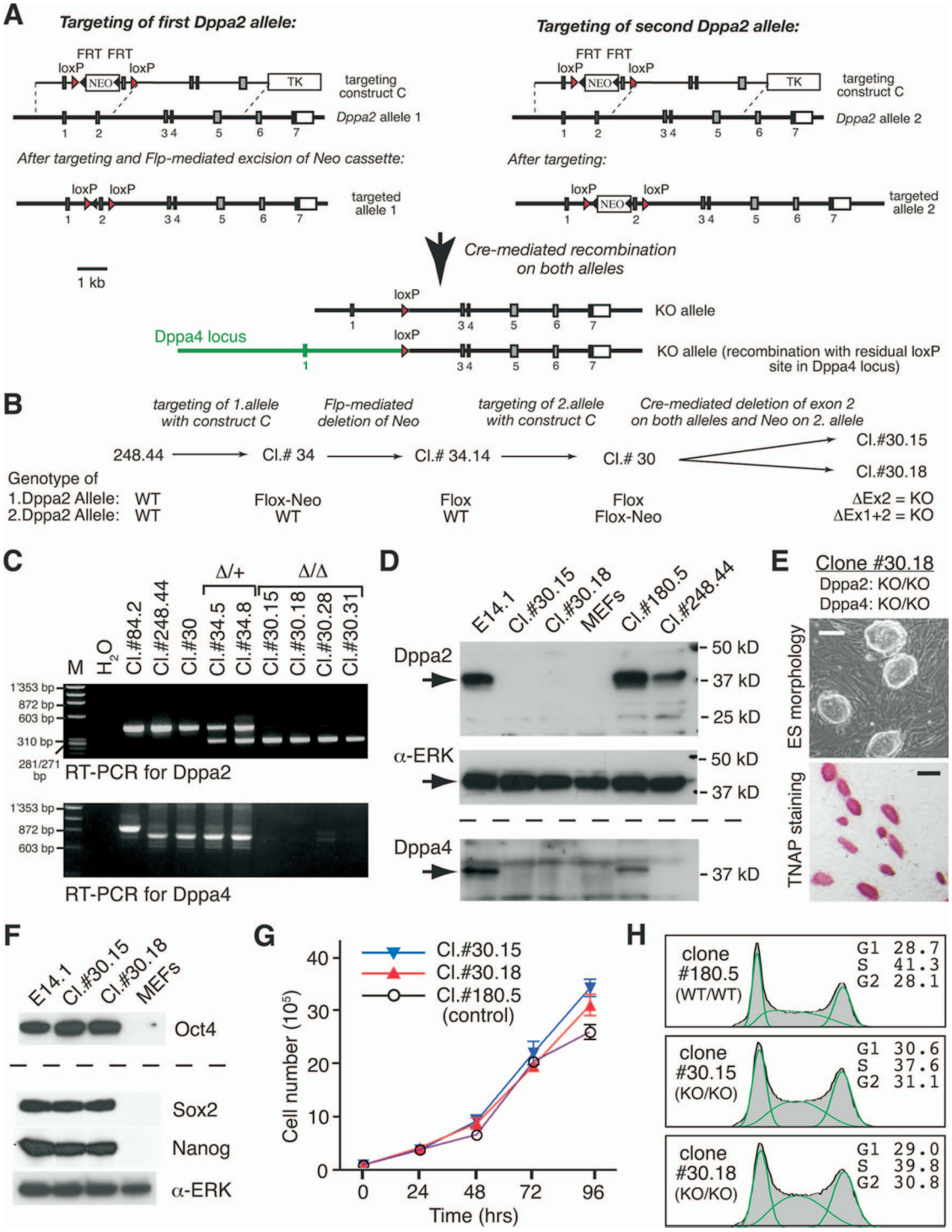

FIG. 4. Homozygous inactivation of *Dppa2* in ES cells lacking Dppa4. (A) Targeting strategy to inactivate both *Dppa2* alleles in ES cells of homozygous Dppa4-deficient clone 248.44. Filled boxes, exons; red triangles, *loxP* sites; black triangles, FRT sites; TK, thymidine kinase cassette for selection against random integration events. After transient Cre expression, the *loxP* sites on one *Dppa2* allele have recombined with the residual *loxP* site in the Dppa4 locus, deleting all sequences in between. (B) Targeting history of the two Dppa2/Dppa4 doubly deficient ES clones 30.15 and 30.18. All manipulations started with clone 248.44 already lacking Dppa4 (Fig. 1). Flox-Neo, allele on which exon 2 has been flanked by *loxP* sites (floxed) and an FRT-flanked Neo selection cassette inserted into intronic sequences upstream of exon 2; Flox, allele on which exon 2 has been flanked by *loxP* sites; ΔEx2, allele on which exon 2 has been deleted; ΔEx1+2, allele on which *loxP* sites flanking the Neo cassette have recombined with the residual *loxP* site in the Dppa4 locus, deleting exons 3 to 7 of Dppa4 and exons 1 and 2 of Dppa2. (C) RT-PCR to detect Dppa2 (top) and Dppa4 (bottom) transcripts in targeted ES clones. Note the absence of functional full-length Dppa2 message (upper band) in homozygous Dppa2-deficient (Δ/Δ) clones 30.12, 30.15, 30.28, and 30.31. In these clones, Dppa4 message is also missing due to insertion of the tdRFP cassette into one *Dppa4* allele and the Cre-mediated recombination event between *Dppa2* and *Dppa4* loci on the other allele. The *Dppa4* genotypes and history of clones 84.2 and 248.44, in which the Dppa2 locus is unmanipulated are shown in Fig. 1B. Clones 34.5 and 34.8 were

for Dppa4 in gene regulation. To probe for potential effects of Dppa4 deficiency on the ES cell transcriptome, we compared global gene expression in wild-type and *Dppa4*$^{-/-}$ ES cells using microarray analysis. To this end, RNA was isolated from Dppa4-deficient and control ES cells (both grown on MEFs in the presence of LIF) and used to probe >39,000 transcripts represented on Affymetrix MOE430 2.0 chips. To allow statistical evaluation of the data, three independent experiments were performed, each with a separately isolated batch of RNA from wild-type as well as knockout ES cells. Although no phenotypically obvious differences between Dppa4-proficient and -deficient ES cells had been apparent (see above), the absence of Dppa4 in ES cells resulted in marked changes in expression levels of a significant number of genes (Fig. 5E and F). When a twofold change in expression was used as an arbitrary cutoff value, transcript levels of 78 nonredundant genes were considered significantly altered. Of these only 2 were upregulated in the absence of Dppa4, while 76 were downregulated (see Table S1 in the supplemental material). Among the genes with lower steady-state transcript levels was Dppa4 itself, most likely indicating that the deletion of exon 2 subjects the resulting frame-shifted, nonfunctional message to nonsense-mediated decay (15). Importantly and in line with our functional analyses reported above, genes like Oct4, Nanog, Sox2, Ronin, or Myc and Klf4, known to be required for (2, 12, 16, 31, 36) or to contribute to (10, 49) ES cell pluripotency/self-renewal were not among the differentially regulated genes. Interestingly, 17 of the 76 identified transcripts (~22%) that were found to be more than twofold downregulated in the absence of Dppa4 encode proteins with established or suggested functions in germ cell development and fertility, among them well-validated genes like Dazl (deleted in azoospermia), Mvh (mouse vasa homolog), Rhox5 (reproductive hox5), or Maelstrom (see Table S2 in the supplemental material). Taken together, our microarray data reveal that loss of Dppa4 in ES cells is not without molecular consequences. In fact, our findings strengthen the hypothesis that Dppa4 is involved in the regulation of gene expression, either at the transcriptional level or by influencing the stability of specific transcripts.

Critical role of Dppa4 in mouse embryogenesis. To probe for in vivo roles of Dppa4, we generated knockout mice via gene targeting. Inactivation of one Dppa4 allele was achieved through homologous recombination in ES cells by replacing exon 2 with the aforementioned tdRFP expression cassette using targeting vector B depicted in Fig. 1A. Heterozygous ES cells from two independently targeted clones (167 and 842) were used to generate chimeric mice, which transmitted the modified Dppa4 locus to offspring. Importantly, the loxP-flanked Neo selection cassette was removed either in vitro by transient expression of Cre recombinase in ES cells of line 167 or in vivo by intercrossing heterozygous mice of line 842 with a universal Cre-deleter mouse (44), giving rise to the "clean" knockout/knock-in allele shown in Fig. 1A (bottom). Correct genetic modification was confirmed in both mouse lines by Southern blot analysis (Fig. 6A). To reduce genetic variability, heterozygous mutant mice of both lines were backcrossed onto the inbred C57BL/6 strain. Unless stated otherwise, all data reported here were obtained with animals of the fifth backcross generation.

Mice heterozygous for the targeted allele were outwardly indistinguishable from wild-type littermates and were obtained at the expected Mendelian ratio in backcrosses with C57BL/6 partners. However, when heterozygote parents were intercrossed, we obtained only 15 homozygous mutants from a total of 687 offspring at the age of weaning (Table 1). This frequency (~2.2%) is more than 10-fold less than the expected Mendelian distribution (25%). Interestingly, mortality was not progressive beyond this point, and the few surviving animals appeared healthy and without obvious defects. For instance, no reduction in body weight was observed in any of the 15 *Dppa4*$^{-/-}$ animals compared with their wild-type or heterozygous littermates. Two homozygous Dppa4-deficient mice, which were sacrificed for a comprehensive analysis of steady-state hemato- and lymphopoiesis by multiparameter flow cytometry, presented all major developmental subpopulations defined by cell surface markers at expected percentages (data not shown). Importantly, there was also no change in the absolute number of thymocytes or the CD4/CD8 subset composition, perturbations of which are generally a good biosensor for stress or disease, and by the time of writing, six homozygous Dppa4-deficient animals had lived beyond 12 months of age without apparent difficulties.

To examine the dramatic loss of *Dppa4*$^{-/-}$ pups, we genotyped embryos from heterozygous parents. As Dppa4 expression is extinguished in all somatic cells at gastrulation (28), we expected to detect consequences of Dppa4 deficiency during early embryogenesis. Surprisingly, when we analyzed four litters at E9.5, we observed no obvious defects (data not shown)

generated by transient expression of Cre recombinase in clone 34 to obtain heterozygous *Dppa2*$^{+/-}$ control cells. (D) Immunoblot of protein extracts from the indicated ES cell clones demonstrating complete absence of Dppa2 protein in clones 30.15 and 30.18, which were derived from Dppa4-deficient clone 248.44. The polyclonal rabbit anti-mouse Dppa2 serum used was directed against an epitope encoded by exon 7. The polyclonal rabbit anti-mouse Dppa4 serum used (lower panel) was the same as described for Fig. 1H. The filter was first hybridized with the anti-Dppa2 antiserum (top) and then stripped and rehybridized with an anti-alpha-ERK antibody (middle) as a loading control. Equal amounts of protein extract were run in parallel on a separate gel for the Dppa4 blot (bottom). The ES cell clones shown have the following Dppa2-Dppa4 genotypes: E14.1, wild type (WT)/WT-WT/WT; clone (Cl) 30.15, knockout (KO)/KO-KO/KO^{RFP}; Cl 30.18, KO/KO-KO/KO^{RFP}; Cl 180.5, WT/WT-Flox/WT; Cl 248.44, WT/WT-KO/KO^{RFP}. (E) Phase contrast microscopy of Dppa2/Dppa4 doubly deficient ES colonies documenting typical ES cell morphology (top) and homogenous expression of the pluripotency marker TNAP. Scale bars, 100 μm (top) and 200 μm (bottom). (F) Immunoblot showing expression of marker proteins (Sox2, Oct4, and Nanog) characteristic for pluripotent cells. (G) No significant difference in proliferation rates between Dppa2/Dppa4 doubly deficient ES cells (clones 30.15 and 30.18) and wild-type ancestor cells (clone 180.5, exon 2 on one *Dppa4* allele floxed). ES cells were plated at 7.5×10^3/ml in duplicate wells and counted at 24-h intervals for 96 h. (H) No significant difference in cell cycle kinetics between Dppa2/Dppa4 doubly deficient ES cells (clones 30.15 and 30.18) and wild-type control cells (clone 180.5). Cells were stained with PI and analyzed by flow cytometry. The percentage of cells in G_1, S, and G_2 phases was determined using the FlowJo cell cycle analysis software Dean/Jett/Fox. α, anti.

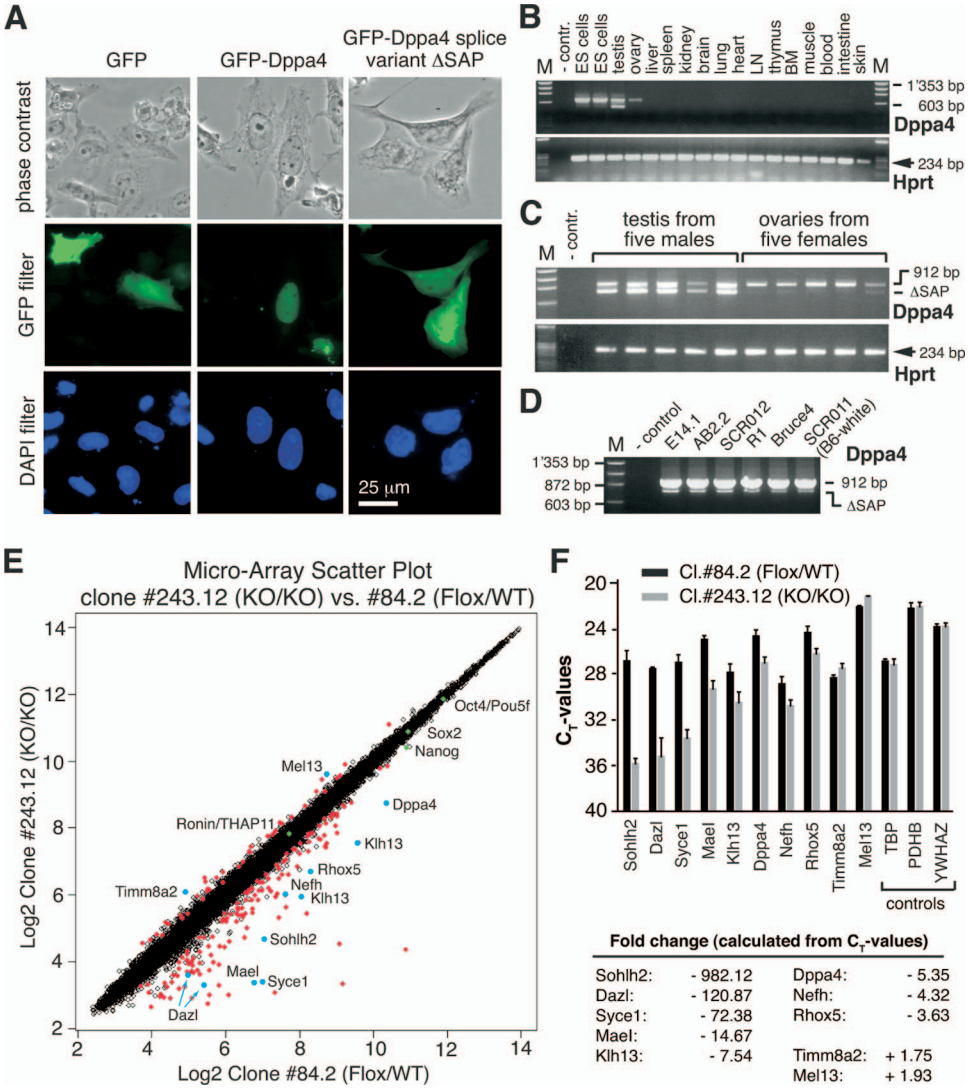

FIG. 5. Effects of Dppa4 deficiency on the ES cell transcriptome. (A) Exclusive localization of full-length Dppa4 to the nucleus is lost in the natural splice variant lacking the SAP domain (Dppa4ΔSAP). Note that the GFP-Dppa4ΔSAP protein lacking the SAP domain diffuses throughout the cell, like the GFP control, while full-length Dppa4 is a nuclear protein (middle panel) (29). GFP fusion constructs were transiently transfected into Panc-1 cells. Lower panels show DAPI staining. In panels B to D RT-PCR analysis of Dppa4 expression demonstrates that message for the natural splice variant lacking the SAP domain is predominantly found in testis. (B) RT-PCR analysis of Dppa4 expression in various tissues from an adult mouse and E14.1 ES cells. M, molecular size marker; −contr, negative control. (C) High levels of Dppa4ΔSAP-encoding message are detected reproducibly by RT-PCR in mouse testis. (D) Generally low levels of Dppa4ΔSAP-encoding message in ES cells, as evidenced by RT-PCR analysis of total RNA from the following six independently derived ES cell lines: E14.1 (25), AB2.2. (41), SCR012 (17), R1 (33), BRUCE4 (24) and SCR011 (from C57BL/6 $tyr^{c\text{-}2J}$ mouse [B6-white]) (Chemicon) (unpublished data). (E) Two-dimensional scatter plot of log ratios of relative transcript levels obtained by Affymetrix microarray analysis. Note the preponderance of downregulated transcripts in the absence of Dppa4 and the unchanged expression levels of Oct4, Sox2, Nanog, and Ronin (green dots) known to be essential for stable maintenance of ES cell identity. The positions of transcripts that were validated by quantitative real-time PCR are marked by blue dots. (F) Validation of Affymetrix GeneChip data for 10 transcripts with altered expression levels by quantitative real-time PCR. TBP (TATA binding box protein), PDHB (pyruvate dehydrogenase E1 component subunit beta mitochondrial precursor), and YWHAZ (14-3-3 protein zeta/delta, or protein kinase C inhibitor protein 1) denote control transcripts with unaltered expression levels. WT, wild type; CT, threshold cycle; KO, knockout; LN, lymph node; BM, bone marrow; Hprt, hypoxanthine phosphoribosyltransferase.

and a Mendelian genotype distribution (Table 1). Although at day E18.5 most *Dppa4*$^{-/-}$ embryos were smaller (Fig. 6B), genotype analysis of more than 380 live embryos at this time point, i.e., a few hours before birth, revealed minimal loss of homozygous Dppa4-deficient animals in line 167 and less than 50% loss in line 842, indicating that the majority of Dppa4-deficient animals die after birth (Table 1). This unexpected result indicates that lethal consequences of Dppa4 deficiency manifest predominantly long after cessation of physiological Dppa4 expression—at least in offspring of heterozygous parents.

Morphological examination of E18.5 embryos lacking Dppa4 revealed additional perplexing findings, which were identical in both lines. While mutant embryos were remarkably

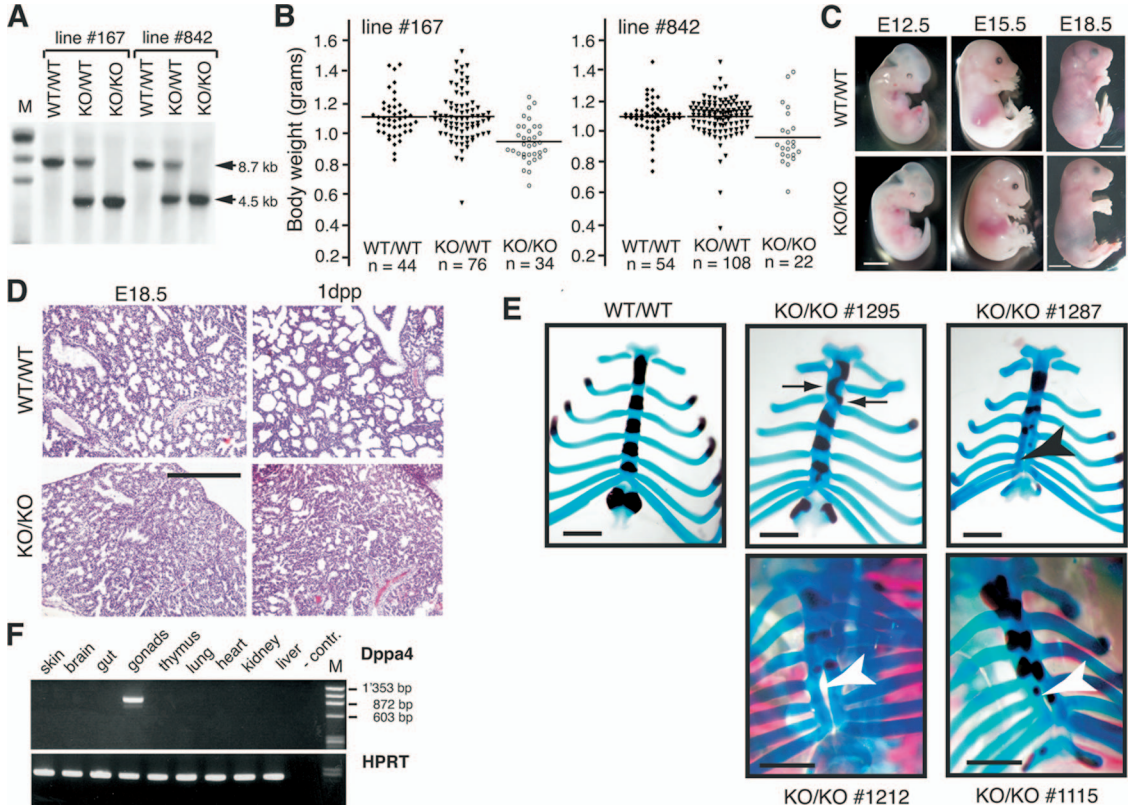

FIG. 6. Developmental defects in Dppa4-deficient mouse embryos and newborns. (A) Southern blot analysis showing expected *Dppa4* banding pattern in both independently generated knockout mouse lines. Genomic DNA from tail biopsies was digested with BglII and hybridized with a 706-bp probe located outside of the targeting construct, which detects a 8.7-kb wild-type and a 4.5-kb null allele (Fig. 1A). Lane M, molecular size marker. (B) Reduced total body weight of homozygous Dppa4-deficient embryos (KO/KO) compared with heterozygous knockout/wild type (KO/WT), and wild-type (WT/WT) littermates on E18.5. Embryos were obtained from timed matings between 10 male and 34 female *Dppa4*$^{+/-}$ parents. Only live embryos are included. (C) Homozygous Dppa4-deficient embryos (KO/KO) and wild-type littermates at different stages of development. Scale bars, 2 mm (E12.5) and 5 mm (E18.5). (D) H&E staining of paraformaldehyde-fixed lung sections from representative homozygous Dppa4-deficient mice (KO/KO) and wild-type littermates. Lung tissue was obtained from live animals on E18.5 or a few hours after birth, as indicated (dpp, day postpartum). Note the striking reduction of alveolar airspace in mutant lungs. Scale bar, 500 μm. (E) Reduced ossification and skeletal dysmorphologies of rib cage in Dppa4-deficient embryos. Skeletons were prepared from embryos at E18.5 and stained with alcian blue for cartilage and alizarin red for bone. Note the reduced ossification of sternebrae and xiphoid processes, the asymmetrical fusion of some ribs to the sternum (black arrows in KO/KO 1295), and abnormal sternal clefts (arrow heads) in Dppa4-deficient animals. Scale bar, 1 mm. (F) No evidence for Dppa4 expression outside of gonadal tissue in a wild-type E15.5 mouse embryo, as determined by sensitive RT-PCR. Lane M, molecular size marker. HRPT, hypoxanthine phosphoribosyltransferase.

normal in their own body proportions (Fig. 6C) and gross organ development, lungs of *Dppa4*$^{-/-}$ embryos and newborns exhibited apparent abnormalities. Histological sections of lung tissue at E18.5 revealed reduced alveolar space, and lungs of the few newborn mutants that could be recovered alive were poorly inflated (Fig. 6D). Most striking, however, was the finding of specific skeletal malformations in *Dppa4*$^{-/-}$ embryos, which were never observed in wild-type or heterozygous littermates. Alcian blue/alizarin red staining of skeletal preps revealed reduced ossification of sternum and ribs in 24 out of 26 homozygous Dppa4-deficient embryos, albeit with various degrees of severity (Fig. 6E). Strikingly, in 7 of the 26 *Dppa4*$^{-/-}$ embryos analyzed, thoracic ribs were fused asymmetrically to the sternum, and four of the mutants exhibited a split xiphisternum extending into a sternal cleft of variable length (Fig. 6E). These very specific skeletal dysmorphologies cannot be explained simply as consequence of a generalized developmental delay in the absence of Dppa4. Most interesting, the defects manifest in somatic tissues, which apparently never expressed Dppa4 (5, 28, 40). In agreement with all published data, we did not detect Dppa4 message by sensitive RT-PCR in any somatic tissue at E15.5 (Fig. 6F), i.e., at the earliest developmental stage when Dppa4-expressing gonads could be dissected away. Our data therefore indicate that Dppa4 activity in pluripotent cells of the pregastrulation embryo is essential for normal development of some somatic tissues, i.e., long after Dppa4 expression has ceased.

Dppa4 is dispensable for germ cell development. After gastrulation, Dppa4 is expressed exclusively in pluripotent cells of the developing germ line (28). We therefore carefully investigated cells and tissues of the reproductive system. Gonads of Dppa4-deficient E12.5 embryos contained germ cells in numbers comparable to those of heterozygous and wild-type littermates (Fig. 7A). Testis and ovaries of the few adult *Dppa4*$^{-/-}$ animals were of normal size and morphology (Fig. 7B), and histological examination did not reveal any abnormalities (Fig.

TABLE 1. Genotypic analysis of offspring from heterozygous × heterozygous breeding pairs

Offspring age and clone line	Total no. of offspring	No. (%) of offspring with Dppa4 genotype[a]		
		+/+	+/−	−/−
Time of weaning[b]				
Line 167[c]	200	68 (34.0)	128 (64.0)	4 (2.0)
Line 842[c]	254	79 (31.1)	172 (67.7)	3 (1.2)
Line 842[d]	233	87 (37.3)	138 (59.2)	8 (3.4)
E18.5				
Line 167[c]	154	44 (28.6)	76 (49.4)	34 (22.0)
Line 842[c]	231	66 (28.6)	133 (57.6)	32 (13.9)
E15.5				
Line 842[c]	171	45 (26.3)	93 (54.4)	33 (19.3)
E9.5				
Line 167[c,e]	34	6 (17.6)	20 (58.8)	8 (23.5)

[a] Cumulative data collected from 95 separate heterozygous × heterozygous breeding pairs.
[b] Weaning, 3 to 4 weeks after birth.
[c] All breeders are fifth generation backcrosses onto C57BL/6 mice.
[d] All breeders are on a mixed (C57BL/6 × 129/Ola)F2 background.
[e] Embryos from four litters.

7C). Ovaries contained follicles at various stages of development, including a number of corpi lutei, and seminiferous tubules of testis and epididymis were filled with sperm. We also determined the relative distribution of germ cell populations in testis using flow cytometric scanning of PI-labeled sperm and detected the three main histogram peaks of DNA content, which correspond to haploid (spermatid and spermatozoa), diploid (spermatogonia, preleptotene primary spermatocytes, and secondary spermatocytes), and tetraploid (spermatogonia, leptotene, zygotene, pachytene, and diplotene primary spermatocytes) cells. No differences in the relative distribution of these maturational subsets were apparent between *Dppa4*$^{-/-}$ and control germ cells (Fig. 7D). In line with histological and flow cytometric data, of the few available homozygous Dppa4-deficient animals, both males and females produced offspring when mice were intercrossed with wild-type littermates (Table 2). However, while male breeders appeared to be fully fertile, one of three test-mated females lacking Dppa4 failed to produce viable offspring, and a second female gave birth to just one viable litter within 12 months (Table 2). Interestingly, none of three intercrosses between homozygous Dppa4-deficient partners resulted in visible pregnancies although *Dppa4*$^{-/-}$ females were found with vaginal plugs, and males were fertile when bred with wild-type partners. Taken together, these observations may hint at a role of Dppa4 as maternal effect gene (see Discussion). Importantly, and in contrast to its specific expression pattern, Dppa4 is clearly not required for development of functional germ cells.

***Dppa4*-driven tdRFP expression is a useful marker for the identification of pluripotent cells and reprogrammed nuclei.** The presence of *Dppa4* transcripts has been exploited repeatedly as a molecular marker for pluripotency (5, 34, 39, 43). The insertion of a tdRFP cassette into the endogenous *Dppa4* locus of ES cells and mice, as described above (Fig. 1A), should permit noninvasive monitoring of Dppa4 expression and direct visualization of pluripotency at the single cell level. As predicted and shown before in this report (Fig. 1F and G), ES cells carrying a tdRFP/Dppa4 knock-in allele exhibit significant red fluorescence. To demonstrate downregulation of tdRFP expression in ES cells losing pluripotency, we performed in vitro differentiation experiments. Using quantitative real-time PCR, Maldonado-Saldivia et al. have shown that Dppa4 message is sharply downregulated in ES cells between day 0 and day 4 of in vitro differentiation (28). In full agreement with this report, we observed a rapid decline in red fluorescence, which was essentially complete after 4 days of differentiation (Fig. 8A). The experiment shown in Fig. 8A was performed with a variant of clone 167ΔNeo (Dppa4 genotype, WT/KO^{RFP}), in which we had additionally targeted a previously described GFP expression cassette (19) into the *Brachyury* gene locus. This double-knock-in ES clone allowed us to visualize at the same time expression of *Dppa4* and of the mesodermal marker gene *Brachyury*, demonstrating both efficient differentiation of ES cells and full compatibility of tdRFP- and GFP-based fluorescent proteins, as reported previously (27).

During embryonic development, Dppa4 is expressed in pluripotent cells of the preimplantation embryo. After gastrulation, Dppa4 expression is confined to male and female primordial germ cells and thereafter to pluripotent cells in testis and ovaries (28). As shown in Fig. 8B, all cells of knock-in preimplantation embryos exhibit red fluorescence, reflecting reported Dppa4 expression. The apparent fluorescence in non-pluripotent trophectoderm cells is most likely due to residual tdRFP protein after the epiblast-trophectoderm lineage split. In line with this interpretation, Dppa2 protein has also been detected in nuclei of trophectoderm cells, despite the absence of strict pluripotency associated Dppa2 message (28). At E12.5, we can easily visualize male and female primordial germ cells based on selective tdRFP expression (Fig. 8C). The intensity of red fluorescence in these cells is sufficiently high to allow their isolation by flow cytometry (Fig. 8D). After gastrulation, we detected red fluorescence exclusively in primordial germ cells and, later in development, in testis and ovaries containing pluripotent cells (Fig. 8E and data not shown). Importantly, in embryos and adult mice, we failed to detect red fluorescent cells in any somatic tissue or cell type outside of testis and ovary, perfectly in line with established Dppa4 expression patterns.

Dppa4 is one of several Oct4-related genes, which are reactivated after transfer of somatic nuclei into enucleated oocytes (5). We therefore tested whether tdRFP expression can be used as a noninvasive marker to monitor successful reprogramming of MEFs into induced pluripotent stem (iPS) cells. After transfection of MEFs carrying the tdRFP/Dppa4 knock-in mutation on one or both alleles with retroviruses encoding the pluripotency-inducing transcription factors OCT4, KLF4, and SOX2 (34), we obtained in a single experiment 22 colonies containing cells with typical ES cell morphology. Two colonies were derived from heterozygous and 20 colonies were from homozygous tdRFP/Dppa4 knock-in MEFs. Importantly, all 22 colonies contained tdRFP-expressing cells in a central area that varied in expanse, indicating reactivation of the Dppa4 locus at least in a subset of reprogrammed cells with apparent ES cell morphology (Fig. 8F). Interestingly, mainly in the rim area of colonies, cells failed to reactivate tdRFP expression

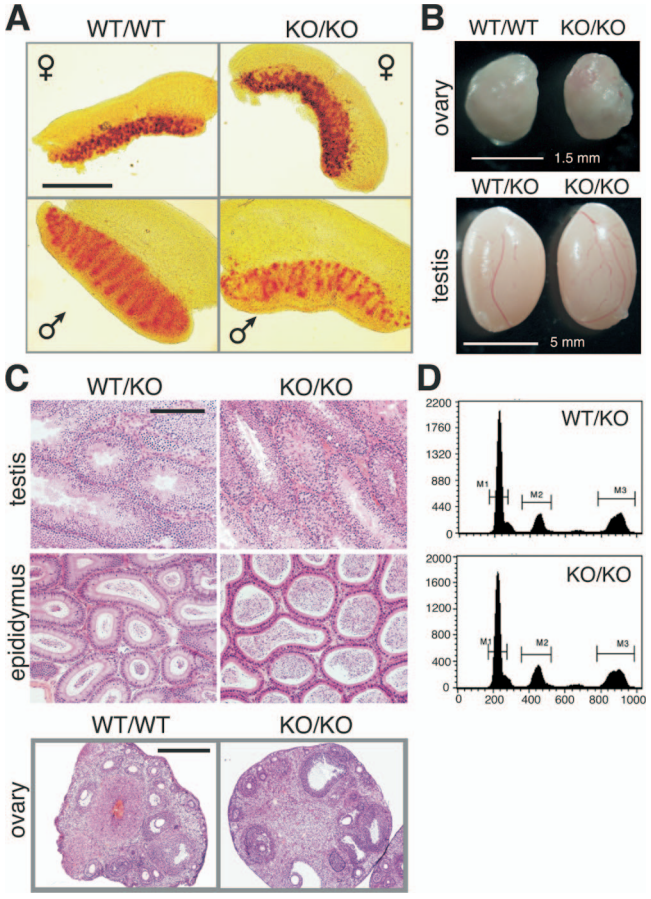

FIG. 7. Efficient germ cell development in mice lacking Dppa4. (A) TNAP staining of gonads from E12.5 embryos to visualize pluripotent germ cells. (B) Unaltered morphology and size of testis and ovaries in adult *Dppa4*$^{-/-}$ mice compared to wild-type littermate controls. (C) H&E-stained paraffin sections of gonads from adult *Dppa4*$^{-/-}$ mice and heterozygous or wild-type littermate controls. Scale bars, 200 μm (testis) and 400 μm (ovaries). (D) Flow cytometric analysis of DNA content in sperm cell suspensions obtained from an adult *Dppa4* null male and a control littermate. M1 represents haploid, M2 represents diploid, and M3 represents tetraploid cells. WT, wild type; KO, knockout.

despite bona fide ES morphology, indicating heterogeneity among reprogrammed cells. In future studies, it may be interesting to characterize tdRFP-positive and -negative populations for potential qualitative differences in their reprogramming status. Nonetheless, our experiment demonstrates robust reactivation of tdRFP expression in a significant fraction of reprogrammed MEFs and, thus, its usefulness as a noninvasive "reprogramming" marker. As homozygous tdRFP/Dppa4 knock-in MEFs are unable to generate functional Dppa4 protein, the outcome of our experiment incidentally provides evidence that Dppa4 activity is dispensable not only for the maintenance of a pluripotent state but also for its efficient induction, at least in iPS cells.

DISCUSSION

Dppa4 has been identified in multiple independent screens as a gene exclusively expressed in pluripotent cells (5, 23, 28, 40, 48), which has led to much speculation about a potential role in maintaining the cellular identity or key characteristics of pluripotent cells. The main incentive of our study was to rigorously assess presumed functions of Dppa4 in ES cell pluripotency and self-renewal and to obtain first insights into its in vivo role. Using gene targeting and *loxP*-Cre technology, we here provide conclusive evidence that Dppa4 is dispensable for the maintenance of a stable pluripotent state in ES cells and in germ cells. Homozygous Dppa4-deficient ES cells preserve their typical morphology; maintain expression of essential and nonessential pluripotency-associated genes, like *Oct4*, *Sox2*, *Nanog*, and *TNAP*; exhibit no alterations in self-renewal capacity; and contribute to cells and tissues of all three germ layers in mouse chimeras. Likewise, we did not detect any defects in germ cell development or function in the absence of Dppa4.

Our findings contradict a recent study in which RNAi was used to investigate the role of Dppa4 in murine ES cells (29). When endogenous *Dppa4* expression was repressed, the authors claimed to observe enhanced differentiation of shRNA-treated ES cells, while the expression of the pluripotency-mediating genes *Oct4* and *Nanog* remained apparently unchanged—a contradiction in itself. Nevertheless, the findings were interpreted to indicate "a requirement of Dppa4 in the maintenance of ES cells in an undifferentiated state." A similar discrepancy between an RNAi and a gene knockout study has recently been reported for *Rex-1*, another pluripotency-associated gene (30). Also, while RNAi experiments would have predicted an essential role of Nanog for the maintenance of ES cells (23), Chambers and colleagues reported recently successful derivation of mutant ES cell lines that were shown to maintain pluripotency and self-renewal capacity, despite constitutive lack of Nanog following targeted inactivation (13). Strong selection of constitutively mutant cells to compensate for permanent gene inactivation is frequently suggested as an ad hoc explanation for differences in phenotype between gene-targeted and RNAi-treated cells. For Dppa4, such an explanation appears highly unlikely as the *loxP*-Cre-based conditional inactivation strategy, which we have chosen, would have unmasked any detrimental effect of Dppa4 deficiency on ES cell identity. Interestingly, a carefully controlled study in which RNAi was successfully employed to identify genes potentially involved in ES cell self-renewal initially also picked

TABLE 2. Breeding performance of individual homozygous Dppa4-deficient mice

Strain or genotype (individual mouse no.)[a]		Duration of mating (mo)	No. of litters (avg litter size[b])
Male	Female		
KO/KO (112)	C57BL/6	8	5 (7)
KO/KO (133)	C57BL/6	6	4 (8)
KO/KO (197)	C57BL/6	11	4 (8)
KO/KO (56)	C57BL/6	7	3 (10)
C57BL/6	KO/KO (135)	6	No offspring
C57BL/6	KO/KO (233)	12	1 (7)
C57BL/6	KO/KO (136)	6	5 (5)
KO/KO (211)	KO/KO (219)	9	No offspring
KO/KO (245)	KO/KO (258)	10	No offspring
KO/KO (264)	KO/KO (276)	8	No offspring

[a] KO, knockout.
[b] Average number of live newborns.

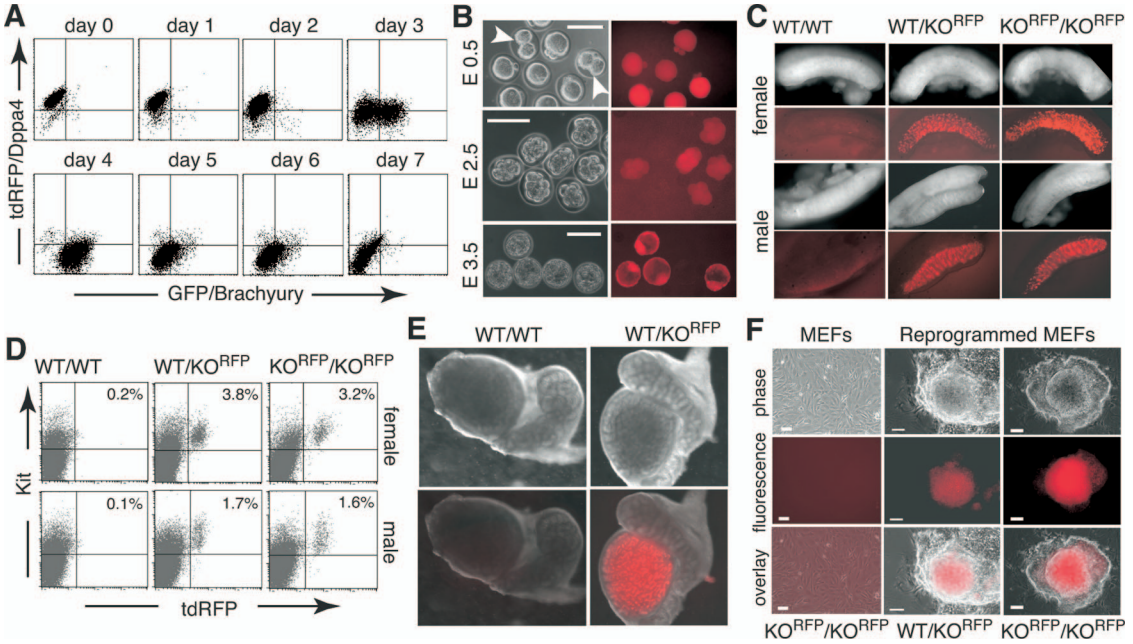

FIG. 8. *Dppa4*-driven tdRFP expression in pluripotent cells. (A) Loss of tdRFP expression in ES cells upon in vitro differentiation. ES cells/embryoid bodies of clone 565 were harvested on the indicated days of differentiation, dissociated, and analyzed by flow cytometry for tdRFP and GFP expression. ES cells of this clone (derived from clone 167ΔNeo by targeting of GFP into the *Brachyury* locus) carry tdRFP in one *Dppa4* allele and a GFP expression cassette in one allele of the *Brachyury* gene locus (19). GFP-*Brachyury* expression serves as a marker for cells that have adopted a mesodermal fate and thus for monitoring correct kinetics of in vitro differentiation. (B) tdRFP expression in preimplantation embryos. The embryos were obtained from timed matings between heterozygous females (WT/KO^{RFP}) and wild-type males (WT/WT). At early stages of development, also embryos with two wild-type alleles exhibit red fluorescence due to expression of maternally deposited tdRFP. The two-cell embryos (white arrowheads), which were obtained from a mating between wild-type C57BL/6 animals, were therefore included as negative control. Scale bar, 150 μm. (C) Strong tdRFP expression in primordial germ cells (PGCs) after colonization of both female and male genital ridges (E12.5). Note the normal number of tdRFP-labeled PGCs in homozygous Dppa4-deficient embryos. (D) PGCs expressing tdRFP can be easily identified and isolated by fluorescence-activated cell sorting. Dot plots show a flow cytometric analysis of cells obtained from dissociated genital ridges of E12.5 embryos. The gender of the animals was determined by PCR. Again, note the normal number of tdRFP-labeled PGCs in homozygous Dppa4-deficient embryos after staining with an anti-kit (anti-CD117) antibody. (E) Expression of tdRFP in testis is localized to developing sperm. Testes and epididymides are from newborn pups. (F) Reactivation of *Dppa4*-driven tdRFP expression in iPS cells generated from tdRFP/Dppa4 knock-in MEFs. MEFs heterozygous or homozygous for the tdRFP/Dppa4 mutation were transfected with retroviruses encoding the pluripotency-inducing factors OCT4, SOX2, and KLF4 (34). The middle and right panels show representative primary colonies 3 to 4 weeks after retroviral transduction of MEFs. Knock-in MEFs used for reprogramming experiments do not exhibit any red fluorescence (left panels). KO, knockout.

out *Dppa4* (23). However, further analysis with additional shRNAs did not rule out off-target effects for the initial Dppa4 shRNA, and inducible expression of Dppa4 did not rescue the differentiating phenotype of the Dppa4 knockdown cells, which is consistent with our findings. Unfortunately, none of these critical control experiments was performed in the study claiming a requirement for Dppa4 (29).

Redundancy with homologous genes is another potential explanation often put forward when gene inactivation does not result in predicted phenotypes. In an electronic search of the mouse genome for *Dppa4*-related sequences, we identified only intronless, truncated and, thus, nonfunctional pseudogenes (data not shown). The closest functional homolog of *Dppa4* is *Dppa2*, a direct neighbor located ~17 kb downstream of *Dppa4* (28). However, indirect and direct evidence argues against a potential role of Dppa2 in compensating for loss of Dppa4. First, our microarray analysis revealed that *Dppa2* transcript levels are not upregulated in the absence of Dppa4, as might have been expected from a gene with compensatory activities. In fact, we find Dppa2 protein is consistently reduced in ES cells lacking Dppa4 (Fig. 4D and data not shown). As *Dppa2* transcript levels are unaltered, this finding may indicate reduced stability or reduced translation of Dppa2 protein in the absence of Dppa4, an observation that merits further investigation. Second, intact *Dppa2* alleles cannot prevent developmental defects and perinatal lethality in homozygous Dppa4-deficient mice. Finally, and probably the most convincing observation, targeted inactivation of both *Dppa2* alleles in ES cells already lacking Dppa4 does not noticeably affect ES cell identity. Of course, our experiments do not exclude the possibility that loss of Dppa4 function in ES cells may be compensated for by some sequence-unrelated gene.

While Dppa4 deficiency in ES cells does not translate into noticeable functional defects, our microarray data reveal clear-cut molecular consequences. In the absence of Dppa4, steady-state levels of 78 nonredundant transcripts were found to be more than twofold altered, with 76 transcripts being downmodulated. Most striking, 17 of the downregulated transcripts (~22%) encode proteins with established or suggested functions in gametogenesis. The strikingly strong representation of gametogenesis-associated transcripts may indicate that Dppa4 is involved in regulating message levels for this functionally

related group of genes. Surprisingly, gametogenesis is not appreciably affected in Dppa4-deficient mice, possibly because residual expression levels of putative target genes are sufficient or because the identified transcripts are less Dppa4-dependent at critical stages of germ cell development. Whether the other identified Dppa4-regulated transcripts play a role in some as yet unknown aspect of ES cell biology or whether their expression is functionally irrelevant for ES cells but may become important for embryonic development later on remains to be investigated, too. Irrespective, the identification of Dppa4-regulated target genes, as reported here, provides a useful starting point for future molecular analyses into the mechanisms of Dppa4 function.

ES cells are sometimes regarded as an in vitro cell type with limited physiological relevance. To assess consequences of Dppa4 deficiency in vivo, we therefore generated knockout mice as well. However, we failed to identify any gross abnormalities in germ cell development, the only cell type with Dppa4 expression after gastrulation. Notably, the few adult *Dppa4*$^{-/-}$ mice, which were obtained from heterozygous parents, contained functional sperm and eggs, which contributed to viable offspring in combination with wild-type gametes. Dppa4 is therefore clearly not required to preserve pluripotency of the germ line. However, deposition of Dppa4 in oocytes may have a critical role during preimplantation development. It is noteworthy that none of three long-term matings between homozygous Dppa4-deficient mice resulted in visible pregnancies (Table 2) although respective males were demonstrably fertile, and females regularly plugged. Fertility of homozygous mutant females appeared to be reduced even in matings with wild-type males although *Dppa4*$^{-/-}$ females are clearly not sterile. While caution is warranted in interpreting findings obtained with so few animals, these observations clearly point to a potential role of *Dppa4* as maternal effect gene. Such a role has recently been documented for *Dppa3*/*Stella*/*Pgc7* (6, 38), another gene encoding a SAP-containing protein with a pluripotency-associated expression pattern. Most embryos derived from Dppa3-deficient oocytes were found arrested in development before the blastocyst stage (6, 38). Homozygous Dppa3-deficient mice were fully viable and were born at Mendelian frequency, which permitted a statistically conclusive affirmation that observed fertility defects were due to a maternal effect. Unfortunately, the paucity of viable homozygote mutant mice permits neither a more extensive evaluation of the breeding performance of *Dppa4*$^{-/-}$ females nor a systematic investigation of potential developmental defects specifically in embryos of homozygous Dppa4-deficient mothers. A conclusive verification of the hypothesis that Dppa4 might act as a maternal effect gene must thus await the generation of fully viable conditional mouse mutants lacking Dppa4 exclusively in the (female) germ line.

In any case, the role of Dppa4 in development is clearly not confined to a putative maternal function as lack of zygotic expression, in contrast to lack of Dppa3/Stella/Pgc7, has drastic developmental consequences. Almost all homozygous Dppa4-deficient mice derived from heterozygous parents die during late embryonic development or within hours after birth. While we do not know the cause of death, poorly inflated lungs may indicate breathing problems as one contributing factor. However, apart from reduced alveolar space, we did not notice any other anatomical defects in Dppa4-deficient lungs, and semiquantitative RT-PCR analysis of a number of transcripts known to be important for normal lung function, like surfactant proteins A, B, C, and D or transcription factors TTF1, Hoxa5, Hoxb5, Sox4, and Sox11, also did not reveal abnormalities (data not shown). The suspected breathing problems may thus be secondary to other, less visible defects.

The two most surprising aspects of Dppa4 deficiency in mice are doubtless the striking skeletal dysmorphologies in rib cage development and the timing of death. As Dppa4 expression outside the germ line is confined to pluripotent cells of the preimplantation embryo, one might have naively expected that consequences of Dppa4 deficiency become apparent early in development. Surely, maternally deposited Dppa4 may mask an essential role of Dppa4 at very early stages of development in embryos derived from heterozygous parents. However, the question remains, how can zygotic Dppa4 deficiency affect the development of somatic tissues, like the skeleton, and lead to death at a time long after cessation of Dppa4 expression in the vast majority of pups? One might argue that insertion of a tdRFP expression cassette in lieu of *Dppa4* exon 2 could cause disturbances within the *Dppa4* chromatin domain, resulting in impaired expression of neighboring genes with a functional role in affected tissues. However, none of the 10 annotated transcripts in the ENSEMBL mouse genome database encoded within 1 Mb upstream (6430553K19Rik) and 1 Mb downstream (Dppa2, Morc1, Trat1, Retnlb, Retnla, Retnlg, Dzip3, C330027C09Rik, and 1700026J12Rik) of the *Dppa4* locus has so far been associated with a function in lung or skeletal tissue or with any other vital role during development. Moreover, our semiquantitative RT-PCR and Affymetrix data indicate that expression of the most proximal gene, *Dppa2*, is not noticeably affected by the genetic modification introduced into the *Dppa4* locus, arguing against nonspecific long-range chromatin effects. Another theoretical explanation that is difficult to rigorously rule out is the possibility of expression of *Dppa4* in somatic precursor cells of affected tissues, perhaps at a very low level or for very brief periods of time. However, a very careful study specifically designed to map *Dppa4* expression could not find any indication of *Dppa4* expression outside pluripotent cells (28), and we could not detect *Dppa4* message by sensitive RT-PCR either in E15.5 embryos outside the gonads (Fig. 6F) or in fluorescently labeled cells in heterozygous or homozygous tdRFP/Dppa4 knock-in embryos at any stage of postgastrulation development, except in pluripotent germ cells and their precursor stages. We therefore consider the striking phenotype in our mice to be most compatible with a role of Dppa4 as a potent epigenetic regulator, which might leave specific marks in the genome that manifest phenotypically at much later stages of development. Although we lack direct evidence for such a hypothesis, recent work on the function of Dppa3 provides an instructive case in point. Molecular analysis of preimplantation embryos from *Dppa3*$^{-/-}$ mothers revealed an essential role of Dppa3 in protecting the maternal genome from demethylation, including several imprinted genes (35). Extensive investigations along this line may eventually unearth related molecular functions for Dppa4. The phenotype of Dppa4-deficient mice reported here thus indicates rewarding directions for further study and provides a suitable starting point. Importantly, we provide conclusive ev-

idence that presumed functions of Dppa4 in maintenance of pluripotency and ES cell self-renewal do not need to be investigated further. Finally, the availability of mice and ES cells that express under the control of Dppa4 a powerful RFP that is fully compatible with widely used GFP-based markers may offer new experimental possibilities for noninvasive detection of pluripotent cells.

ACKNOWLEDGMENTS

We thank Manja Thorwirth, Nathalie Schöler, and Franziska Beckel for mouse genotyping; Franziska Beckel for reliable technical assistance; R. Syhachak for expert care of the mouse colony; and Hans-Reimer Rodewald for many helpful discussions. All microarray processing steps and data analysis were performed at the Microarray Facility Tübingen, and we thank M. Walter, Tübingen, for professional support.

This work has been supported by Landesforschungsschwerpunkt: Molekulare Mechanismen zur Aufrechterhaltung des Stammzellcharakters and Sonderforschungsbereich SFB497-A7.

REFERENCES

1. **Aravind, L., and E. V. Koonin.** 2000. SAP—a putative DNA-binding motif involved in chromosomal organization. Trends Biochem. Sci. **25:**112–114.
2. **Avilion, A. A., S. K. Nicolis, L. H. Pevny, L. Perez, N. Vivian, and R. Lovell-Badge.** 2003. Multipotent cell lineages in early mouse development depend on SOX2 function. Genes Dev. **17:**126–140.
3. **Babaie, Y., R. Herwig, B. Greber, T. C. Brink, W. Wruck, D. Groth, H. Lehrach, T. Burdon, and J. Adjaye.** 2007. Analysis of Oct4-dependent transcriptional networks regulating self-renewal and pluripotency in human embryonic stem cells. Stem Cells **25:**500–510.
4. **Benyamini, Y., and Y. Hochberg.** 1995. Controlling the false discovery rate: a practical and powerful approach to multiple testing. J. R. Stat. Soc. B **57:**289–300.
5. **Bortvin, A., K. Eggan, H. Skaletsky, H. Akutsu, D. L. Berry, R. Yanagimachi, D. C. Page, and R. Jaenisch.** 2003. Incomplete reactivation of Oct4-related genes in mouse embryos cloned from somatic nuclei. Development **130:** 1673–1680.
6. **Bortvin, A., M. Goodheart, M. Liao, and D. C. Page.** 2004. *Dppa3*/*Pgc7*/*stella* is a maternal factor and is not required for germ cell specification in mice. BMC Dev. Biol. **4:**2.
7. **Boyer, L. A., T. I. Lee, M. F. Cole, S. E. Johnstone, S. S. Levine, J. P. Zucker, M. G. Guenther, R. M. Kumar, H. L. Murray, R. G. Jenner, D. K. Gifford, D. A. Melton, R. Jaenisch, and R. A. Young.** 2005. Core transcriptional regulatory circuitry in human embryonic stem cells. Cell **122:**947–956.
8. **Buchholz, F., P. O. Angrand, and A. F. Stewart.** 1998. Improved properties of FLP recombinase evolved by cycling mutagenesis. Nat. Biotechnol. **16:** 657–662.
9. **Campbell, R. E., O. Tour, A. E. Palmer, P. A. Steinbach, G. S. Baird, D. A. Zacharias, and R. Y. Tsien.** 2002. A monomeric red fluorescent protein. Proc. Natl. Acad. Sci. USA **99:**7877–7882.
10. **Cartwright, P., C. McLean, A. Sheppard, D. Rivett, K. Jones, and S. Dalton.** 2005. LIF/STAT3 controls ES cell self-renewal and pluripotency by a Myc-dependent mechanism. Development **132:**885–896.
11. **Chakravarthy, H., B. Boer, M. Desler, S. K. Mallanna, T. W. McKeithan, and A. Rizzino.** 2008. Identification of DPPA4 and other genes as putative Sox2:Oct-3/4 target genes using a combination of in silico analysis and transcription-based assays. J. Cell Physiol. **216:**651–662.
12. **Chambers, I., D. Colby, M. Robertson, J. Nichols, S. Lee, S. Tweedie, and A. Smith.** 2003. Functional expression cloning of Nanog, a pluripotency sustaining factor in embryonic stem cells. Cell **113:**643–655.
13. **Chambers, I., J. Silva, D. Colby, J. Nichols, B. Nijmeijer, M. Robertson, J. Vrana, K. Jones, L. Grotewold, and A. Smith.** 2007. Nanog safeguards pluripotency and mediates germline development. Nature **450:**1230–1234.
14. **Chambers, I., and A. Smith.** 2004. Self-renewal of teratocarcinoma and embryonic stem cells. Oncogene **23:**7150–7160.
15. **Chang, Y. F., J. S. Imam, and M. F. Wilkinson.** 2007. The nonsense-mediated decay RNA surveillance pathway. Annu. Rev. Biochem. **76:**51–74.
16. **Dejosez, M., J. S. Krumenacker, L. J. Zitur, M. Passeri, L. F. Chu, Z. Songyang, J. A. Thomson, and T. P. Zwaka.** 2008. Ronin is essential for embryogenesis and the pluripotency of mouse embryonic stem cells. Cell **133:**1162–1174.
17. **Deng, T., Y. Kuang, D. Zhang, L. Wang, R. Sun, G. Xu, Z. Wang, and J. Fei.** 2007. Disruption of imprinting and aberrant embryo development in completely inbred embryonic stem cell-derived mice. Dev. Growth Differ. **49:** 603–610.
18. **Evans, M.** 2005. Embryonic stem cells: a perspective. Novartis Found. Symp. **265:**98–103; discussion 103–106, 122–128.
19. **Fehling, H. J., G. Lacaud, A. Kubo, M. Kennedy, S. Robertson, G. Keller, and V. Kouskoff.** 2003. Tracking mesoderm induction and its specification to the hemangioblast during embryonic stem cell differentiation. Development **130:**4217–4227.
20. **Ginsburg, M., M. H. Snow, and A. McLaren.** 1990. Primordial germ cells in the mouse embryo during gastrulation. Development **110:**521–528.
21. **Goossens, K., M. Van Poucke, A. Van Soom, J. Vandesompele, A. Van Zeveren, and L. J. Peelman.** 2005. Selection of reference genes for quantitative real-time PCR in bovine preimplantation embryos. BMC Dev. Biol. **5:**27.
22. **Hellemans, J., G. Mortier, A. De Paepe, F. Speleman, and J. Vandesompele.** 2007. qBase relative quantification framework and software for management and automated analysis of real-time quantitative PCR data. Genome Biol. **8:**R19.
23. **Ivanova, N., R. Dobrin, R. Lu, I. Kotenko, J. Levorse, C. DeCoste, X. Schafer, Y. Lun, and I. R. Lemischka.** 2006. Dissecting self-renewal in stem cells with RNA interference. Nature **442:**533–538.
24. **Kontgen, F., G. Suss, C. Stewart, M. Steinmetz, and H. Bluethmann.** 1993. Targeted disruption of the MHC class II Aa gene in C57BL/6 mice. Int. Immunol. **5:**957–964.
25. **Kuhn, R., K. Rajewsky, and W. Muller.** 1991. Generation and analysis of interleukin-4 deficient mice. Science **254:**707–710.
26. **Loh, Y. H., J. H. Ng, and H. H. Ng.** 2008. Molecular framework underlying pluripotency. Cell Cycle **7:**885–891.
27. **Luche, H., O. Weber, T. Nageswara Rao, C. Blum, and H. J. Fehling.** 2007. Faithful activation of an extra-bright red fluorescent protein in "knock-in" Cre-reporter mice ideally suited for lineage tracing studies. Eur. J. Immunol. **37:**43–53.
28. **Maldonado-Saldivia, J., J. van den Bergen, M. Krouskos, M. Gilchrist, C. Lee, R. Li, A. H. Sinclair, M. A. Surani, and P. S. Western.** 2007. Dppa2 and Dppa4 are closely linked SAP motif genes restricted to pluripotent cells and the germ line. Stem Cells **25:**19–28.
29. **Masaki, H., T. Nishida, S. Kitajima, K. Asahina, and H. Teraoka.** 2007. Developmental pluripotency-associated 4 (DPPA4) localized in active chromatin inhibits mouse embryonic stem cell differentiation into a primitive ectoderm lineage. J. Biol. Chem. **282:**33034–33042.
30. **Masui, S., S. Ohtsuka, R. Yagi, K. Takahashi, M. S. Ko, and H. Niwa.** 2008. Rex1/Zfp42 is dispensable for pluripotency in mouse ES cells. BMC Dev. Biol. **8:**45.
31. **Mitsui, K., Y. Tokuzawa, H. Itoh, K. Segawa, M. Murakami, K. Takahashi, M. Maruyama, M. Maeda, and S. Yamanaka.** 2003. The homeoprotein Nanog is required for maintenance of pluripotency in mouse epiblast and ES cells. Cell **113:**631–642.
32. **Murry, C. E., and G. Keller.** 2008. Differentiation of embryonic stem cells to clinically relevant populations: lessons from embryonic development. Cell **132:**661–680.
33. **Nagy, A., J. Rossant, R. Nagy, W. Abramow-Newerly, and J. C. Roder.** 1993. Derivation of completely cell culture-derived mice from early-passage embryonic stem cells. Proc. Natl. Acad. Sci. USA **90:**8424–8428.
34. **Nakagawa, M., M. Koyanagi, K. Tanabe, K. Takahashi, T. Ichisaka, T. Aoi, K. Okita, Y. Mochiduki, N. Takizawa, and S. Yamanaka.** 2008. Generation of induced pluripotent stem cells without Myc from mouse and human fibroblasts. Nat. Biotechnol. **26:**101–106.
35. **Nakamura, T., Y. Arai, H. Umehara, M. Masuhara, T. Kimura, H. Taniguchi, T. Sekimoto, M. Ikawa, Y. Yoneda, M. Okabe, S. Tanaka, K. Shiota, and T. Nakano.** 2007. PGC7/Stella protects against DNA demethylation in early embryogenesis. Nat. Cell Biol. **9:**64–71.
36. **Nichols, J., B. Zevnik, K. Anastassiadis, H. Niwa, D. Klewe-Nebenius, I. Chambers, H. Scholer, and A. Smith.** 1998. Formation of pluripotent stem cells in the mammalian embryo depends on the POU transcription factor Oct4. Cell **95:**379–391.
37. **Niwa, H.** 2007. How is pluripotency determined and maintained? Development **134:**635–646.
38. **Payer, B., M. Saitou, S. C. Barton, R. Thresher, J. P. Dixon, D. Zahn, W. H. Colledge, M. B. Carlton, T. Nakano, and M. A. Surani.** 2003. Stella is a maternal effect gene required for normal early development in mice. Curr. Biol. **13:**2110–2117.
39. **Pritsker, M., N. R. Ford, H. T. Jenq, and I. R. Lemischka.** 2006. Genome-wide gain-of-function genetic screen identifies functionally active genes in mouse embryonic stem cells. Proc. Natl. Acad. Sci. USA **103:**6946–6951.
40. **Ramalho-Santos, M., S. Yoon, Y. Matsuzaki, R. C. Mulligan, and D. A. Melton.** 2002. "Stemness": transcriptional profiling of embryonic and adult stem cells. Science **298:**597–600.
41. **Ramirez-Solis, R., P. Liu, and A. Bradley.** 1995. Chromosome engineering in mice. Nature **378:**720–724.
42. **Rasmussen, R.** 2001. Quantification on the LightCycler. Rapid cycle real-time PCR, methods and applications. Springer Press, Heidelberg, Germany.
43. **Ruau, D., R. Ensenat-Waser, T. C. Dinger, D. S. Vallabhapurapu, A. Rolletschek, C. Hacker, T. Hieronymus, A. M. Wobus, A. M. Muller, and M. Zenke.** 2008. Pluripotency associated genes are reactivated by chromatin-modifying agents in neurosphere cells. Stem Cells **26:**920–926.
44. **Schwenk, F., U. Baron, and K. Rajewsky.** 1995. A cre-transgenic mouse

strain for the ubiquitous deletion of loxP-flanked gene segments including deletion in germ cells. Nucleic Acids Res. **23:**5080–5081.
45. **Shimshek, D. R., J. Kim, M. R. Hubner, D. J. Spergel, F. Buchholz, E. Casanova, A. F. Stewart, P. H. Seeburg, and R. Sprengel.** 2002. Codon-improved Cre recombinase (iCre) expression in the mouse. Genesis **32:** 19–26.
46. **Silva, J., and A. Smith.** 2008. Capturing pluripotency. Cell **132:**532–536.
47. **Smyth, G. K.** 2004. Linear models and empirical bayes methods for assessing differential expression in microarray experiments. Stat. Appl. Genet. Mol. Biol. **3:**Article 3.
48. **Sperger, J. M., X. Chen, J. S. Draper, J. E. Antosiewicz, C. H. Chon, S. B. Jones, J. D. Brooks, P. W. Andrews, P. O. Brown, and J. A. Thomson.** 2003. Gene expression patterns in human embryonic stem cells and human pluripotent germ cell tumors. Proc. Natl. Acad. Sci. USA **100:**13350–13355.
49. **Takahashi, K., and S. Yamanaka.** 2006. Induction of pluripotent stem cells from mouse embryonic and adult fibroblast cultures by defined factors. Cell **126:**663–676.
50. **Vigneau, C., K. Polgar, G. Striker, J. Elliott, D. Hyink, O. Weber, H. J. Fehling, G. Keller, C. Burrow, and P. Wilson.** 2007. Mouse embryonic stem cell-derived embryoid bodies generate progenitors that integrate long term into renal proximal tubules in vivo. J. Am. Soc. Nephrol. **18:**1709–1720.